Neuro
-endocrinology

DOI: 10.1159/000499693
Received: 11/14/2018
Accepted: 3/17/2019
Published(online): 3/20/2019

GLP-1-, but not GDF-15-, receptor activation increases the number of IL-6-expressing cells in the external lateral parabrachial nucleus

Anesten F. Mishra D. Dalmau Gasull A. Engström-Ruud L. Bellman J. Pálsdóttir V. Zhang F.-P. Trapp S. Skibicka K.P. Poutanen M. Jansson J.-O.

ISSN: 0028-3835 (Print), eISSN: 1423-0194 (Online)
https://www.karger.com/NEN
Neuroendocrinology

GLP-1-, but not GDF-15-, receptor activation increases the number of IL-6-expressing cells in the external lateral parabrachial nucleus

Fredrik Anesten[1], Devesh Mishra[1,2], Adrià Dalmau Gasull[1], Linda Engström-Ruud[1], Jakob Bellman[1], Vilborg Palsdottir[1], Fu-Ping Zhang[3], Stefan Trapp[4], Karolina P. Skibicka[1,2], Matti Poutanen[3], John-Olov Jansson[1]

Affiliations

[1] Department of Physiology, Institute of Neuroscience and Physiology, The Sahlgrenska Academy at the University of Gothenburg, S-413 45 Gothenburg, Sweden

[2] Wallenberg Centre for Molecular and Translational Medicine, Gothenburg, Sweden

[3] Institute of Biomedicine, Research Centre for Integrative Physiology and Pharmacology, and Turku Center for Disease Modeling, University of Turku, Kiinamyllynkatu 10, FI-20520 TURKU, Finland

[4] Centre for Cardiovascular and Metabolic Neuroscience, Department of Neuroscience, Physiology & Pharmacology, University College London, London, WC1E 6BT, UK

Correspondence should be addressed to:
Prof. John-Olov Jansson
joj@neuro.gu.se
Medicinaregatan 11
Box 432
40530 Gothenburg, Sweden
031-786 3526

Key words: hindbrain, RedIL6, immunohistochemistry, in-situ hybridization, interleukins

List of non-standard abbreviations

CGRP – calcitonin gene related peptide
Ex4 – exendin-4
GDF15 – growth and differentiation factor 15
GFRAL – GDNF family receptor alpha-like
GLP-1 – glucagon like peptide 1
GLP-1R – glucagon like peptide 1 receptor
IL-6Rα – interleukin-6 receptor alpha
MIC1 – macrophage inhibitory cytokine 1
NTS – nucleus of the solitary tract
PBN – parabrachial nucleus
PBNel – external lateral parabrachial nucleus
RFP – red fluorescent protein
STAT3 – signal transducer and activator of transcription 3

Abstract

IL-6 in the hypothalamus and hindbrain is an important downstream mediator of suppression of body weight and food intake by glucagon-like peptide-1 (GLP-1) receptor stimulation. CNS GLP-1 is produced almost exclusively in prepro-glucagon neurons in the nucleus of the solitary tract. These neurons innervate energy balance-regulating areas, such as the external lateral parabrachial nucleus (PBNel); essential for induction of anorexia.

Using a validated novel IL-6-reporter mouse strain, we investigated the interactions in PBNel between GLP-1, IL-6 and calcitonin gene related peptide (CGRP, a well-known mediator of anorexia). We show that PBNel GLP-1R-containing cells highly (to about 80%) overlap with IL-6-containing cells on both protein and mRNA level.

Intraperitoneal administration of a GLP-1 analogue exendin-4 to mice increased the proportion of IL-6 containing cells in PBNel 3-fold, while there was no effect in the rest of the lateral PBN. In contrast, injections of an anorexigenic peptide growth and differentiation factor 15 (GDF15) markedly increased the proportion of CGRP-containing cells, while IL-6-containing cells were not affected.

In summary, GLP-1R are found on IL-6 producing cells in PBNel, and GLP-1R stimulation leads to an increase in the proportion of cells with IL-6 reporter fluorescence, supporting IL-6 mediation of GLP-1 effects on energy balance.

Introduction

Interleukin-6 (IL-6) is a cytokine with important roles in both pro-inflammatory and anti-inflammatory responses. Expressed together with pro inflammatory cytokines, such as TNF-α, IL-6 may have deleterious effects on metabolism [1-3]. On the other hand, when interacting with hormones with metabolically stimulating effects such as glucagon like peptide-1 (GLP-1), IL-6 seems to accentuate their effects on metabolism [4-8]. It is known that this multifunctional cytokine has widespread sites of synthesis, being produced in immune cells, adipose tissue and skeletal muscle during exercise, but also in the CNS [4, 9-12].

The clinical implications of stimulation and inhibition of the IL-6 receptor alpha (IL-6Rα) is a topic of ongoing studies [13]. IL-6Rα is located outside the CNS, but also in many CNS regions, including many of the fundamental energy-regulatory hypothalamic and hindbrain nuclei [14-20]. Much is known about the exact localization of IL-6Rα thanks to the availability of well validated antibodies against IL-6Rα itself [15-17] and against markers of IL-6Rα activation such as pSTAT3 [21]. Conversely, due to lack of validated antibodies considerably less is known about production of IL-6 in the CNS, including in the hindbrain, a part of the CNS that also has been shown to be important in regulation of metabolism [22, 23].

IL-6 has been proved to have an important role in body weight regulation. Previous studies in IL-6 $^{-/-}$ mice with phenotypic mature-onset obesity have shown that IL-6 inhibits obesity via effects in CNS [24]. This assumption is supported by the fact that intracerebroventricular injections of IL-6, but not peripheral injections, cause weight-reducing effects by means of increased energy expenditure [25, 26] presumably via phosphorylation of STAT3 [14]. Furthermore, it is likely that pathologically high IL-6 release contributes to cachexia development [1, 27, 28], since blocking IL-6 synthesis in several mouse cancer models attenuates the progression of the wasting syndrome [29, 30].

The parabrachial nucleus (PBN) is essentially formed by two different sub-nuclei. The medial PBN (mPBN) (which) integrates signals associated with gustatory properties of food, as well as cardiovascular- and thermo-regulation. The lateral PBN instead has been shown to be important for anorexigenic signaling [31-33]. Lately, one part of the lateral PBN, the external lateral PBN (PBNel) has received special attention [31, 34]. The PBNel receives direct projections from neurons of the nucleus of the solitary tract (NTS) [23], and projects to other important centers for the regulation of metabolic activity, such as different parts of the hypothalamus and the amygdala [35-37]. Recent studies by us and others have indicated that hindbrain glucagon-like peptide 1 (GLP-

1) producing neurons project to the lateral PBN, including PBNel, and that stimulation of lateral PBN GLP-1R by GLP-1 agonist exendin-4 (Ex4) reduces food intake and body weight in rats. Furthermore, this lateral PBN GLP-1R stimulation by Ex4 increases the gene expression of IL-6 and calcitonin gene-related peptide (CGRP), both of which are energy balance regulating peptides and potent downstream mediators of GLP-1R activation [38]. However, the relation between IL-6 and CGRP in the PBNel is largely unknown.

Recently, there has been a large interest for the finding that the growth and differentiation factor 15 (GDF15, also known as macrophage inhibitory cytokine-1, MIC-1) interacts with the PBNel [39] to decrease food intake. GDF15 is released from peripheral tissues during disease, and serum GDF15 has been regarded as a biomarker of various disease states [40]. Recently, the receptor for GDF15, GFRAL, was identified and shown to be present to a large extent in the area postrema and NTS, areas known to mediate signals, including those of illness, from the periphery to the CNS [39, 41-43].

In the present study we investigated the effects of the two anorectic factors GLP-1 and GDF15 on the anorectic and cachectic brain area PBNel. We especially investigated the effect of GLP-1 and GDF15 on IL-6 and CGRP, two well-known anorectic factors produced in the PBNel. The identification of IL-6 producing cells was enabled using a newly generated IL-6-reporter mouse strain. We also investigated if IL-6 is present in GLP-1R-containing cells, allowing for a direct stimulation of IL-6 production by GLP-1 in the PBNel.

Materials and Methods

Animals

To study IL-6 protein expression *in vivo* in a reporter mouse, cDNA coding for a red fluorescent protein mKate2 was inserted into IL6 gene locus (Fig. S1), exactly after the translation start site, ATG. For further details on how these reporter mice were generated and validated, see supplementary information. In order to visualize IL-6 we used 12-week-old male and female heterozygous mice expressing far-red fluorescent protein (mKATE2) under the control of the IL-6 promoter. In order to visualize GLP-1R, we used a GLP-1R reporter mouse strain. For further details on this strain, see [44].

Animals had *ad libitum* access to water and standard chow pellets (Tekland Global, Harlan, The Netherlands), and were kept under standardized conditions (12 h light/dark cycle (lights on at 6:00 AM), 50-60% humidity,

24-26ºC temperature). The local ethics committee for animal care at the University of Gothenburg approved all animal procedures.

Tissue preparation for immunohistochemistry

For experiments on how GLP-1R and GFRAL-stimulation affect RedIL6-fluorescence, exendin-4 (1933; RnD Systems Inc, Minneapolis, MA, USA (3 mg/kg)) or recombinant human GDF15 (9279; RnD Systems Inc, Minneapolis, MA, USA (1 mg/kg)) was intraperitoneally administered to RedIL6-mice thirty minutes before sacrifice. NaCl was used as a control. In the other experiments, the mice were untreated before sacrifice. Following injection or no treatment, mice were deeply anaesthetized and perfused transcardially with heparinized saline (50 IU/ml) followed by 4% paraformaldehyde in 0.1M phosphate buffer. Brains were removed and post fixed in 4% paraformaldehyde in 0.1M phosphate buffer containing 15% sucrose over night at 4 °C. They were then transferred to a 30% sucrose solution in 0.1M phosphate buffer until sectioning. Coronal 20µm thick serial sections of the hypothalamus and hindbrain were cut using a Leica CM3050S cryostat (Leica Microsystem, Wetzlar, Germany) and stored in cryoprotectant solution (25% ethylene glycol; 25% glycerol; 0.1 M phosphate buffer). Coronal sections corresponding to bregma -5,07 to -5.41, interneural -1.28 to -1.62 [45] were selected for staining.

Immunohistochemistry

Briefly, sections were rinsed in wash buffer (0.1M TrisHCl, pH 7.5, 0.15M NaCl) and blocked for 1 h with Tris-NaCl-Boehringer milk powder (TNB) with 0.2% Triton-X-100 (Perkin Elmer, Waltham, MA, USA). Sections were incubated with primary antibodies (Table 1) 48h at 4 °C. After rinsing, sections were incubated for 1 h with secondary antibodies (Table 1) diluted in TNB blocking reagent with 0.2% Triton-X-100. Sections were then rinsed and stained with either Alexa Fluor 488, 568 or 594 (Table 1). After a further wash, cell nuclei were stained with DAPI (1:5000, D1306; ThermoFisher Scientific, Waltham, MA , USA) for 15 min, rinsed and mounted in mounting medium containing prolong diamond anti fade (P36965; ThermoScientific). As a control for unwanted cross-reactivity for the secondary antibodies, some sections were incubated with mismatching primary and secondary antibodies, resulting in negative staining. Antibodies, their dilutions and catalogue numbers, as well as the manufacturers providing them are listed in Table 1. Four mice per treatment group and experiment [no treatment (Fig 1-2), Ex-4 and vehicle (Fig 3-4), GDF-15 and vehicle (Fig 5-6)] were used for

immunohistochemistry. Cell counting was performed from one brain slice from each of the four animals. Representative confocal micrographs from these animals were used to construct figures.

Confocal microscopy and cell counting

Images of the stained sections were obtained using either a confocal microscope system (LSM 700; ZEISS, Oberkochen, Germany), together with a Plan APO ×40 A/1.40 oil lens (for close-up pictures) or a Plan Fluor ×20/0.75 lens (for anatomical overview pictures) and a solid-state laser. For co-localization between IL-6 mKATE2 (stained with an anti-RFP antibody) and CGRP respectively, focus stacking was used to achieve a greater depth of field and as such make it possible to more accurately detect possible co-localization.

PBNel RFP-labelled cells, CGRP immunoreactive cells and co-staining between RFP- and IL-6 antibody-immunoreactive cells was quantified from at least four 20 µm thick sections per brain. Cells that stained positively for mKATE2-, CGRP-ab and/or GLP-1R-reporter immunoreactivity are defined as IL-6-, CGRP- and/or GLP-1R-containing cells, respectively. The proportional difference in immunoreactivity was obtained by dividing antibody-immunoreactive cells by the amount of DAPI-immunoreactive cell nuclei in the plane of focus. Cell counting data was analyzed using student's t-test.

Triple channel confocal images (to cover the entire PBNel) were generated with a Plan Fluor ×20/0.75 lens and a solid-state laser. A tile scan of 4x4 tiles was obtained from the centre of the lateral PBN, covering the entire nucleus. Neurons were considered labelled when the staining was clearly above background. The emission spectrum of the secondary fluorescent antibody is well known.

By adjusting the beam splitter of the confocal microscope, the signal of the fluorophore was maximized while minimizing background fluorescence. The evaluation of cell labelling was done with the cell nucleus in the plane of focus. A total of four slides were counted per experiment, each from a different male or female mouse, and the average of two separate counts per slide was taken. Counting was performed without knowledge of what treatment the animal had received.

Micrographs were adjusted for brightness and contrast in FIJI [46] and tile scan overviews were constructed using a FIJI plug-in [47].

RNA-scope

For RNAscope lateral PBN containing brain sections (12 µm thick) were cut and fixed in 10% formalin (ThermoFisher scientific, Waltham, MA, USA) for 30 min. Following 2 quick washes in PBS, brain slices were dehydrated in 50% (5 min), 70% (5 min) and twice in 100% (5 min each) ethanol and then treated with protease solution (pretreatment IV) at room temperature for 30 minutes. The protease was washed away with PBS. Target probe for GLP-1R (Rn-GLP-1R 315221-C1), IL-6 (Rn-IL-6-C3 427141-C3) and negative control probes were applied directly on the sections to cover them completely and incubated at 40°C for 2 h in the HybEZ oven. Then, preamplifier and amplifier probes were added (AMP1, 40°C for 30 min; AMP2, 40°C for 15 min; AMP3, 40°C for 30 min; AMP4-Alt C for 15 min). Finally, brain sections were incubated for 30 seconds with DAPI and mounting medium for fluorescence (VECTASHIELD, Vector Laboratories, Burlingame, CA, USA). Fluorescent images of the lateral PBN were captured at 40x using LSM700 Zeiss confocal microscope and images were processed using Zen lite software.

Statistics

Graphs were constructed using GraphPad Prism 8 (GraphPad Software, San Diego, CA, USA). Statistical analyses were made using Students t-test and $p < 0.05$ was considered significant.

Results

Validation of "RedIL6" mKATE2-IL-6 reporter mouse

To validate the mKATE2/IL-6 reporter, we compared the reporter mouse staining with IL-6 immunoreactivity in wild type mice. For this, we used a comercial polyclonal anti-IL-6 antibody that showed little immunostaining in IL-6-/- mice [9]. Co-staining with this antibody in mKATE2/IL-6 mice, "RedIL6 mice", showed that almost all cells in PBNel visualized in the RedIL6 reporter mouse were also stained by the antibody (Fig 1A-B). Moreover, almost all cells containing IL-6-antibody immunoreactivity were also visualized by the RedIL6 reporter construct (Fig 1A-B). In conclusion, the present results show that two completely different strategies to visualize IL-6 stain the same cells. This is in line with the assumption that the RedIL6 reporter mouse staining show *bona fide* IL-6-containing cells.

IL-6- immunoreactivity and GLP-1R-fluorescence and mRNA overlap to a large extent in lateral PBN

Sections from GLP-1R reporter mice were stained with an RFP antibody and co-stained with the anti-IL-6 antibody described above to detect co-staining between GLP-1R and IL-6 (Fig 2). Red tdRFP immunoreactivity, reflecting presence of GLP-1R, was present in cells throughout the PBNel, as was IL-6-immunoreactivity (Fig 2A-B). Cell counting showed that the majority of the GLP-1R containing cells were also IL-6-immunoreactive (80%) (Fig 2C), whereas the proportion of IL-6-containing cells that were also GLP-1R positive was lower (44%) (Fig 2D). In line with this, many cells in the lateral PBN expressing GLP-1R mRNA also expressed IL-6 mRNA as indicated by fluorescent in situ hybridization (RNA-scope) (Fig 2E-F).

Intraperitoneal injection of the GLP-1 analogue Ex-4 increased the proportion of IL-6- and CGRP-containing cells in PBNel

Slices from RedIL6 reporter mice were used to determine the proportion of cells containing IL-6 after intraperitoneal injection of either Ex-4 (3 mg/kg) (Fig 3A-B) or NaCl (Fig 3C-D). Cell counting showed that 44% of PBNel cells contained IL-6 30 min after Ex-4 injection whereas a smaller proportion, 13%, contained IL-6 after vehicle-injection (Fig 3E). Similar results were obtained 60 min after Ex4 injection (Fig S5). There appeared to be no effect of Ex-4 on the proportion of IL-6 containing cells in other parts of the lateral PBN (Fig 3E). Thus, the GLP-1 analogue Ex-4 appears to cause a three-fold increase in the proportion of IL-6 containing cells in the PBNel.

Intraperitoneal injection of Ex4 increased the proportion of CGRP-containing cells to a lesser degree than Ex4 increased IL-6 (Fig 4A-E). The proportion of cells that contained CGRP was 31% after Ex4 and 24% after vehicle (Fig 4E). There appears to be no effect on other parts of the lateral PBN (Fig 4E). Thus, the effect of Ex4 on IL-6 protein seems to be larger than the effect on CGRP protein. This is consistent with our previous findings that Ex4 increases IL-6 mRNA in PBN to a many times greater degree than CGRP mRNA [38]. There appears to be some overlap between RedIL6 fluorescence and CGRP-immunoreactivity where about 40% of CGRP cells also showed RedIL6 fluorescence. Similarly, about 40 % of RedIL6 fluorescent cells also showed CGRP-immunoreactivity (Fig S3A-B).

The number of DAPI-immunoreactive cells was constant in both treated and control groups in both experiments, implying that the increase in RedIL6 and CGRP-fluorescence was not due to proliferation of cells.

Intraperitoneal injection of GDF15 increases the proportion of CGRP-, but not IL-6-containing cells in PBNel

Slices from RedIL6 reporter mice were used to identify IL-6 containg cells after intraperitoneal injection of either GDF15 (1 mg/kg) or vehicle (NaCl).There was no difference in the proportion of IL-6 containing cells in the PBNel for GDF15-infused mice (Fig 5A-B) as compared with vehicle treated controls (Fig 5C-D), as confirmed by cell counting (Fig 5E). There was no difference in IL-6 cells between GDF15- and vehicle-infused mice in any other subnucleus of the lateral PBN (Fig 5E).

In brains stained with CGRP-antibody, GDF15 induced a clearly larger proportion of CGRP containng cells (Fig 6A-B) compared to vehicle treatment (Fig 6C-D). Cell counting showed that about 56% of cells in PBNel showed CGRP-immunoreactivity after GDF15-injection compared to only 27% for the vehicle treated control mice, i.e. a 2-fold increase induced by GDF15 (Fig 6E). There was no difference in CGRP between GDF15- and vehicle-infused mice in any other subnucleus of the lateral PBN (6E). The proportion of CGRP-containing cells in other subnuclei of PBN was unchanged compared with controls (not shown). Thus, GDF15 appears to increase the proportion of CGRP-containg cells (Fig 6A-E) , but not of IL-6- containing cells (Fig 5A-E) in PBNel.

Discussion

Development and validation of the novel mKATE2/IL-6 reporter mouse strain "RedIL6"

The field of IL-6 research has been hampered by the lack of well recognized and reliable antibodies against this peptide; antibodies that could be used e g for visualization of IL-6, not least in a complex organ such as the brain. Thus, we developed a knock-in reporter mouse strain that expresses a red fluorescent protein, mKATE2, in IL-6-expressing cells. This mouse strain, on a C57/B6 background, with mKATE2 under the control of the IL-6 promoter was named the "RedIL6" reporter mouse. The assumption that the novel reporter mouse strain is a *bona fide* IL-6 reporter is supported by several findings. i) The construct itself was validated in several different ways during its development, as reported in Supplementary Information. ii) We show that the cells in RedIL6 mice also contain mouse IL-6 m RNA, as detected by RNA scope (Suppl Fig 3). iii) We found that almost all cells in the PBNel with RedIL6-fluorescence also showed IL-6-immunoreactivity using a previously published anti –IL-6 polyclonal antibody. iv) This antibody has been reported to display little staining in IL-6-/- mice [9]. Moreover, we obtained a similar decrease in IL-6 immunoreactivity in another mouse model of IL-6

knockout, the homzygous RedIL6, which has mKATE2 knock-in into both IL-6 gene alleles (not shown), supporting the specificity of this antibody for IL-6. The almost complete overlap between IL-6 containing cells detected by the RedIL6 construct and the antibody, indicates that two very different techniques to detect IL-6 resulted in identification of largely the same cells. The simplest explanation for these results is that the cells detected both by the reporter construct and the antibody are *bona fide* IL-6-containing cells.

Interactions between IL-6 and GLP-1 in PBNel

We here show that systemic treatment with the GLP-1 analogue Ex-4 can increase the number of IL-6 containing cells in PBN, mainly in the external subdivision of this nucleus, PBNel. We also show that there is a large overlap between IL-6 and GLP-1R-immunoreactivity in the PBNel and that this overlap is also present at the mRNA-level. This is in line with previous results that Ex4 enhances IL-6 mRNA levels in the PBN [38]. GLP-1 originating in the brain is almost exclusively produced by prepro-glucagon (PPG) neurons of the NTS which then project to, among other nuclei, the PBN [7, 38, 48, 49].

Our working hypothesis is that GLP-1 fibers from NTS PPG-neurons could reach GLP-1R-containing cells in the PBNel which in turn release IL-6 (Fig 7). IL-6 could then act as a downstream mediator of GLP-1 on energy balance. We have previously shown that IL-6Rα is present on PPG-neurons and that IL-6 can activate these neurons, partially via increased Ca2+-inflow [14]. The present findings in the PBNel strengthen our hypothesis that IL-6 is an important downstream mediator of GLP-1 effects on energy metabolism in the hypothalamus and the hindbrain as a whole [50].

In the present study we found that Ex4 increased the proportion of cells with RedIL6 fluorescence already after 30-60 min, which is a surprisingly rapid effect. However, it has been reported that peripheral Ex4 treatment can exert more rapid effects on the brain than GLP-1 itself [51]. Possible explanations may include rapid translation from existing mRNA, a decrease of neuronal IL-6 secretion and/or axonal transport. Future experiments are needed to determine what gives rise to this surprisingly rapid increase in RedIL6 fluorescence. The effect is unlikely to be a reporter mouse artefact since Ex4 and GDF15 induced a similar rapid induction of CGRP immunoreactivity in wild type mice. The increased proportion of fluorescent cells is also in line with other findings such as Ex4 increased IL-6 and Calca mRNA [38] and GDF15 induced c-Fos in CGRP neurons [39].

The effect of Ex-4 on the number of IL-6 expressing cells may seem surprisingly high considering the fact that 80% of the GLP-1R expressing cells already contain IL-6 in untreated control brains. There could be several possibilities for this; firstly, the co-localization of GLP-1R and IL-6 may be less in other projections of the PBNel. However, it seems very unlikely to be less than 30% which would give room for a three-fold

increase in the number of IL-6 expressing cells in the subpopulation of cells that also express GLP-1R. Secondly, there may be an effect in cells that have levels of GLP-1R that are under the detectable limit. Thirdly, GLP-1 may indirectly increase the IL-6 expression in cells that do not contain GLP-1R.

It may seem logical and obvious to inhibit IL-6 in the PBNel to investigate GLP-1 responsiveness, but there may be problems. One is that IL-6 detected in cell bodies of PBN is likely to be transported in axons to nerve terminals in other parts of the brain. In the parts of the brain that receive projections from PBN, it may be possible to neutralize effects of GLP-1 stimulated IL-6 release, while it is less likely to happen in the PBN itself. The IL-6Rα in PBN may be auto receptors that inhibit the release of IL-6, and thereby the IL-6 mediated effects of GLP-1. IL-6 has been shown to regulate its own production in an autocrine manner outside the CNS [52]. Alternatively, the IL-6Rα may mediate a feed forward effect. In conclusion, the effects of IL-6 blockade in PBNel may be difficult interpret, and best studied in a separate paper.

Possible interactions between CGRP and GLP-1 in PBNel

CGRP is regarded as the major player when it comes to regulation of energy balance and anorexia in the PBNel [34, 53]. The results of the present study suggest that intraperitoneal injection of Ex4 slightly increases CGRP protein levels, as measured by cell counting, on micrographs of immunostained brain sections. This is in line with a previous report that intracerebroventricular infusion of Ex4 increases CGRP-mRNA levels in the lateral PBN [38]. Interestingly, there appears to be a partial overlap between neurons containing IL-6 and CGRP in the PBNel (Fig S3A-B). Future studies are needed to investigate if GLP-1 acts in PBNel via two different downstream mediators, CGRP and IL-6, produced in two different cell types to exercise its effects on energy balance. Alternatively, CGRP and IL-6 from the same cells could act in tandem as downstream mediators of GLP-1R stimulation. Finally, there could be combination of the two possibilities described above.

Effects by GDF15 on IL-6 and CGRP in PBNel

Recently, GFRAL was identified as the receptor for the cachectic circulating factor GDF15 and found to be located almost exclusively in the area postrema and the NTS of the hindbrain [39, 41-43]. This finding sparked a large interest, given that area postrema is a chemo trigger center believed to mediate cachectic and anorectic signals from the periphery to the CNS. Published data suggests that there is a little interplay between GDF15 and GLP-1 [39, 41-43], despite the fact that GLP-1, like GDF15, is believed to act via area postrema and NTS to decrease appetite and body fat [49, 54]. More excitingly, it has been shown that peripheral injection of GDF15 leads to c-fos activation in CGRP neurons in the PBNel [39]. This ties in with the results in this paper

that peripheral GDF15-injection increased CGRP-immunoreactivity in PBNel. In contrast, RedIL6-fluorescence was unchanged by GDF15. Thus, GDF15 may exert its anorectic effects via CGRP but not IL-6. IL-6 and CGRP are produced in cells that contain IL-6 only, CGRP only, or both in the PBNel. IL-6 and CGRP may be two separate downstream mediators of the effects on energy balance exerted by GLP-1 and GDF15, respectively (see Fig 7).

Conclusions

In this paper, we show data supporting that IL-6 can act as a downstream mediator of GLP-1-effects on energy balance in the PBNel. Using a validated novel reporter mouse strain, the mKATE2-IL-6-mouse "RedIL6", we show that IL-6 is present in cells of the PBNel, and that the proportion of IL-6 containing cells is increased after peripheral injection of the GLP-1 analogue Ex4. Using a GLP-1R-reporter mouse model, we also show that IL-6 antibody-immunoreactivity is found in most GLP-1R containing cells. The results obtained with the in-situ hybridization technique further strengthens these data, showing that GLP-1R- and IL-6-mRNA are largely found in the same cells, enabling direct effects by Ex4 on IL-6 containing cells. In contrast, the GDF15-GFRAL system did not affect IL-6 in PBNel. In line with previous results, GFD15 enhanced the proportion of CGRP containing PBNel cells. Taken together, we here show data that further support the GLP-1-IL-6 system as an important player in PBNel for regulation of energy balance.

Acknowledgements

We thank Erik Schéle for the schematic illustration of the key findings of the paper. We thank the Centre for Cellular Imaging at the University of Gothenburg and the National Microscopy Infrastructure, NMI (VR-RFI 2016-00968) for the use of imaging equipment, as well as support received from Julia Fernandez-Rodriguez, Maria Smedh and Carolina Tängemo. We also thank the personnel at Turku Center for Disease Modeling (www.tcdm.fi) for skillful technical assistance in generating the reporter mouse line for IL-6. This work was supported by the NovoNordisk Foundation, the Swedish Research Council, the Swedish Government [under the Avtal om Läkarutbildning och Medicinsk Forskning (Agreement for Medical Education and Research)], the Knut and Alice Wallenberg Foundation, EC Framework 7, and the Torsten Söderbergs Foundation (to JOJ) and by the Swedish Research Council (2014-2945 to KPS), Wallenberg Foundation (to KPS), Novo Nordisk Foundation Excellence project grant (to KPS), and Ragnar Söderberg Foundation (KPS). Medical Research Council (MRC) grant MR/N02589X/1 (to ST).

Author Contributions

F.A and J.O.J designed research; F.A, J.O.J, S.T and K.P.S analyzed data; F.A, D.M, A.D.G and J.B performed research; F.A, A.D.G and J.O.J wrote the paper; L.E.R, V.P, F.P.S, M.P and S.T contributed new analytical tools.

References

1 Hodge D, Hurt E, Farrar W: The role of IL-6 and STAT3 in inflammation and cancer. European journal of cancer 2005;41:2502-2512.
2 Ishihara K, Hirano T: IL-6 in autoimmune disease and chronic inflammatory proliferative disease. Cytokine & growth factor reviews 2002;13:357-368.
3 Sundgren-Andersson AK, Ostlund P, Bartfai T: IL-6 is essential in TNF-alpha-induced fever. The American journal of physiology 1998;275:R2028-2034.
4 Le Foll C, Johnson MD, Dunn-Meynell AA, Boyle CN, Lutz TA, Levin BE: Amylin-induced central IL-6 production enhances ventromedial hypothalamic leptin signaling. Diabetes 2015;64:1621-1631.
5 Steensberg A, van Hall G, Osada T, Sacchetti M, Saltin B, Klarlund Pedersen B: Production of interleukin-6 in contracting human skeletal muscles can account for the exercise-induced increase in plasma interleukin-6. The Journal of physiology 2000;529 Pt 1:237-242.
6 Timper K, Denson JL, Steculorum SM, Heilinger C, Engstrom-Ruud L, Wunderlich CM, Rose-John S, Wunderlich FT, Bruning JC: IL-6 Improves Energy and Glucose Homeostasis in Obesity via Enhanced Central IL-6 trans-Signaling. Cell reports 2017;19:267-280.
7 Llewellyn-Smith I, Reimann F, Gribble F, Trapp S: Preproglucagon neurons project widely to autonomic control areas in the mouse brain. Neuroscience 2011;28:111-121.
8 Sadagurski M, Norquay L, Farhang J, D'Aquino K, Copps K, White M: Human IL6 enhances leptin action in mice. Diabetologia 2010;53:525–535.
9 Aniszewska A, Chłodzińska N, Bartkowska K, Winnicka M, Turlejski K, Djavadian R: The expression of interleukin-6 and its receptor in various brain regions and their roles in exploratory behavior and stress responses. Journal of Neuroimmunology 2015;15:1-9.
10 Mauer J, Denson JL, Bruning JC: Versatile functions for IL-6 in metabolism and cancer. Trends in immunology 2015;36:92-101.
11 Hidalgo J, Florit S, Giralt M, Ferrer B, Keller C, Pilegaard H: Transgenic mice with astrocyte-targeted production of interleukin-6 are resistant to high-fat diet-induced increases in body weight and body fat. Brain, Behavior and Immunity 2010;24:119-126.
12 Wedell-Neergaard A, Lang Lehrskov L, Højgaard Christensen R, Elster Legaard G, Dorph E, Korsager Larsen M, Launbo N, Ravn Fagerlind S, Kofoed Seide S, Nymand S, Ball M, Vinum N, Noerfelt Dahl C, Henneberg M, Ried-Larsen M, Damm Nybing J, Christensen R, Rosenmeier J, Karstoft K, Klarlund Pedersen B, Ellingsgaard H, Krogh-Madsen R: Exercise-Induced Changes in Visceral Adipose Tissue Mass Are Regulated by IL-6 Signaling: A Randomized Controlled Trial. Cell Metabolism 2018:30744-30747.

13 Lehrskov LL, Lyngbaek M, Soederlund L, Legaard G, Ehses J, Heywood S, Wewer Albrechtsen N, Holst J, Karstoft K, Pedersen B, Ellingsgaard H: Interleukin-6 Delays Gastric Emptying in Humans with Direct Effects on Glycemic Control. Cell Metabolism 2018;27:1201-1211.
14 Anesten F, Holt MK, Schéle E, Pálsdóttir V, Reimann F, Gribble F.M, Safari C, Skibicka K.P, Trapp S, J.O J: Preproglucagon neurons in the hindbrain have IL-6 receptor-α and show Ca2+ influx in response to IL-6. American Journal of Physiology Regulative Integrative Comparative Physiology 2016;311:R115-123.
15 Benrick A, Schéle E, Pinnock S, Wernstedt-Asterholm I, Dickson S, Karlsson-Lindahl L, Jansson JO: Interleukin-6 gene knockout influences energy balance regulating peptides in the hypothalamic paraventricular and supraoptic nuclei. Journal of Neuroendocrinology 2009;21:620-628.
16 Schéle E, Benrick A, Grahnemo L, Egecioglu E, Anesten F, Pálsdóttir V, Jansson JO: Inter-relation between interleukin (IL)-1, IL-6 and body fat regulating circuits of the hypothalamic arcuate nucleus. Journal of Neuroendocrinology 2013;25:580-589.
17 Schéle E, Fekete C, Egri P, Füzesi T, Palkovits M, Keller É, Liposits Z, Gereben B, Karlsson-Lindahl L, Shao R, Jansson JO: Interleukin-6 receptor α is co-localised with melanin-concentrating hormone in human and mouse hypothalamus. Journal of Neuroendocrinology 2012;24:930-943.
18 Matthews V, Allen T, Risis S, Chan M, Henstridge D, Watson N, Zaffino L, Babb J, Boon J, Meikle P, Jowett J, Watt M, Jansson J, Bruce C, Febbraio M: Interleukin-6-deficient mice develop hepatic inflammation and systemic insulin resistance. Diabetologia 2010;53:2431-2441.
19 Pedersen BK, Febbraio M: Muscle as an endocrine organ: focus on muscle-derived interleukin-6. Physiological Reviews 2008;88:1379-1406.
20 Yuen D, Dwyer R, Matthews V, Zhang L, Drew B, Neill B, Kingwell B, Clark M, Rattigan S, Febbraio M: Interleukin-6 Attenuates Insulin-Mediated Increases in Endothelial Cell Signaling but Augments Skeletal Muscle Insulin Action via Differential Effects on Tumor Necrosis Factor-α Expression. Diabetes 2009;58:1086–1095.
21 Orellana D, Quintanilla R, Gonzalez-Billault C, Maccioni R: Role of the JAKs/STATs pathway in the intracellular calcium changes induced by interleukin-6 in hippocampal neurons. Neurotoxicity Research 2005;8:295-304.
22 Skibicka K, Grill H: Hypothalamic and hindbrain melanocortin receptors contribute to the feeding, thermogenic, and cardiovascular action of melanocortins. Endocrinology 2009:5351–5361.
23 Norgren R, Leonard CM: Taste pathways in rat brainstem. Science 1971;173:1136-1139.
24 Wallenius V, Wallenius K, Ahren B, Rudling M, Carlsten H, Dickson SL, Ohlsson C, Jansson JO: Interleukin-6-deficient mice develop mature-onset obesity. Nature medicine 2002;8:75-79.
25 Wallenius K, Wallenius V, Sunter D, Dickson SL, Jansson JO: Intracerebroventricular interleukin-6 treatment decreases body fat in rats. Biochemical and biophysical research communications 2002;293:560-565.
26 Wallenius K, Jansson JO, Wallenius V: The therapeutic potential of interleukin-6 in treating obesity. Expert opinion on biological therapy 2003;3:1061-1070.
27 Cahlin C, Korner A, Axelsson H, Wang W, Lundholm K, Svanberg E: Experimental cancer cachexia: the role of host-derived cytokines interleukin (IL)-6, IL-12, interferon-gamma, and tumor necrosis factor alpha evaluated in gene knockout, tumor-bearing mice on C57 Bl background and eicosanoid-dependent cachexia. Cancer research 2000;60:5488-5493.
28 Strassmann G, Fong M, Kenney JS, Jacob CO: Evidence for the involvement of interleukin 6 in experimental cancer cachexia. The Journal of clinical investigation 1992;89:1681-1684.
29 Ando K, Takahashi F, Kato M, Kaneko N, Doi T, Ohe Y, Koizumi F, Nishio K, Takahashi K: Tocilizumab, a proposed therapy for the cachexia of Interleukin6-expressing lung cancer. PloS one 2014;9:e102436.
30 Garbers C, Heink S, Korn T, Rose-John S: Interleukin-6: designing specific therapeutics for a complex cytokine. Nature Reviews Drug Discovery 2018;17:395-412.

31 Carter M, Soden M, Zweifel L, Palmiter R: Genetic identification of a neural circuit that suppresses appetite. Nature 2013;503:111-114.
32 Mraovitch S, Kumada M, Reis D: Role of the nucleus parabrachialis in cardiovascular regulation in cat. Brain Research 1982;232:57-75.
33 Hermann G, Rogers R: Convergence of vagal and gustatory afferent input within the parabrachial nucleus of the rat. Journal of the Autonomic Nervous System 1985;13:1-17.
34 Campos C, Bowen A, Schwartz M, Palmiter R: Parabrachial CGRP Neurons Control Meal Termination. Cell Metabolism 2016;23:811-820.
35 Anderberg R, Anefors C, Bergquist F, Nissbrandt H, Skibicka K: Dopamine signaling in the amygdala, increased by food ingestion and GLP-1, regulates feeding behavior. Physiology and Behavior 2014;136:135-144.
36 Cole S: Changes in the feeding behavior of rats after amygdala lesions. Behavioral Biology 1974;12:265-270.
37 Molero-Chamizo A: Modulation of the magnitude of conditioned taste aversion in rats with excitotoxic lesions of the basolateral amygdala. Neurobiology of Learning and Memory 2017;137:56-64.
38 Richard J, Farkas I, Anesten F, Anderberg RH, Dickson S, Gribble FM, Reimann F, Jansson JO, Liposits Z, Skibicka KP: GLP-1 receptor stimulation of the lateral parabrachial nucleus reduces food intake: neuroanatomical, electrophysiological, and behavioral evidence. Endocrinology 2014;155:4356-4367.
39 Hsu J, Crawley S, Chen M, Ayupova D, Lindhout D, Higbee J, Kutach A, Joo W, Gao Z, Fu D, To C, Mondal K, Li B, Kekatpure A, Wang M, Laird T, Horner G, Chan J, McEntee M, Lopez M, Lakshminarasimhan D, White A, Wang S, Yao J, Yie J, Matern H, Solloway M, Haldankar R, Parsons T, Tang J, Shen W, Alice Chen Y, Tian H, Allan B: Non-homeostatic body weight regulation through a brainstem-restricted receptor for GDF15. Nature 2017;550:255-259.
40 Yang Y, Yan S, Tian H, Bao Y: Macrophage inhibitory cytokine-1 versus carbohydrate antigen 19-9 as a biomarker for diagnosis of pancreatic cancer: A PRISMA-compliant meta-analysis of diagnostic accuracy studies. Medicine (Baltimore) 2018;97:e9994.
41 Emmerson P, Wang F, Du Y, Liu Q, Pickard R, Gonciarz M, Coskun T, Hamang M, Sindelar D, Ballman K, Foltz L, Muppidi A, Alsina-Fernandez J, Barnard G, Tang J, Liu X, Mao X, Siegel R, Sloan J, Mitchell P, Zhang B, Gimeno R, Shan B, Wu X: The metabolic effects of GDF15 are mediated by the orphan receptor GFRAL. Nature Medicine 2017;23:1215-1219.
42 Mullican S, Lin-Schmidt X, Chin C, Chavez J, Furman J, Armstrong A, Beck S, South V, Dinh T, Cash-Mason T, Cavanaugh C, Nelson S, Huang C, Hunter M, Rangwala S: GFRAL is the receptor for GDF15 and the ligand promotes weight loss in mice and nonhuman primates. Nature Medicine 2017;23:1150-1157.
43 Yang L, Chang C, Sun Z, Madsen D, Zhu H, Padkjær S, Wu X, Huang T, Hultman K, Paulsen S, Wang J, Bugge A, Frantzen J, Nørgaard P, Jeppesen J, Yang Z, Secher A, Chen H, Li X, John L, Shan B, He Z, Gao X, Su J, Hansen K, Yang W, Jørgensen S: GFRAL is the receptor for GDF15 and is required for the anti-obesity effects of the ligand. Nature Medicine 2017;23:1158-1166.
44 Cork S, Richards J, Holt M, Gribble F, Reimann F, Trapp S: Distribution and characterisation of Glucagon-like peptide-1 receptor expressing cells in the mouse brain. Molecular Metabolism 2015;4:718-731.
45 Paxinos G, Franklin K: Paxinos and Franklin's the Mouse Brain in Stereotaxic Coordinates 4th Edition. Academic Press, 2012.
46 Schindelin J, Arganda-Carreras I, Frise E, Kaynig V, Longair M, Pietzsch T, Preibisch S, Rueden C, Saalfeld S, Schmid B, Tinevez J, White D, Hartenstein V, Eliceiri K, Tomancak P, Cardona A: Fiji: an open-source platform for biological-image analysis. Nature Methods 2012;9:676-682.
47 Preibisch S, Saalfeld S, Tomancak P: Globally optimal stitching of tiled 3D microscopic image acquisitions. Bioinformatics 2009;25:1463-1465.

48 Grill H, Hayes M: Hindbrain neurons as an essential hub in the neuroanatomically distributed control of energy balance. Cell Metabolism 2012;16:296-309.
49 Hayes MR, Skibicka KP, Grill HJ: Caudal brainstem processing is sufficient for behavioral, sympathetic, and parasympathetic responses driven by peripheral and hindbrain glucagon-like-peptide-1 receptor stimulation. Endocrinology 2008;149:4059-4068.
50 Shirazi R, Palsdottir V, Collander J, Anesten F, Vogel H, Langlet F, Jaschke A, Schürmann A, Prévot V, Shao R, Jansson JO, Skibicka KP: Glucagon-like peptide 1 receptor induced suppression of food intake and body weight is mediated by central IL-1 and IL-6. PNAS 2013;110:16199-16204.
51 Labouesse M, Stadlbauer U, Weber E, Arnold M, Langhans W, Pacheco-López G: Vagal afferents mediate early satiation and prevent flavour avoidance learning in response to intraperitoneally infused exendin-4. Journal of Neuroendocrinology 2012;24:1505–1516.
52 Verboogen D, Revelo N, Ter Beest M, van den Bogaart G: Interleukin-6 secretion is limited by self-signaling in endosomes. Journal of Molecular Cell Biology 2018:Epub ahead of print.
53 Campos C, Bowen A, Han S, Wisse B, Palmiter R, Schwartz M: Cancer-induced anorexia and malaise are mediated by CGRP neurons in the parabrachial nucleus. Nature Neuroscience 2017;20:934-942.
54 Kanoski SE, Fortin SM, Arnold M, Grill HJ, Hayes MR: Peripheral and central GLP-1 receptor populations mediate the anorectic effects of peripherally administered GLP-1 receptor agonists, liraglutide and exendin-4. Endocrinology 2011;152:3103-3112.

Figure 1. RedIL6-fluorescence and IL-6 antibody immunoreactivity overlap to a large extent in PBNel

Figure 1 shows overlap between cells with IL-6 antibody immunoreactivity (green) and RedIL6-immunoreactivity (red). Cell nuclei (blue) are stained by DAPI (A). Yellow arrowheads show examples of co-localization. Cell counting shows a large overlap between the two different methods for detecting IL-6 immunoreactivity where roughly 95% of cells that were positive for RedIL6 were also IL-6 antibody immunoreactive (B). Confocal micrographs were obtained and cell counting was performed as described in Materials and Methods. Scale bars 80 μm (overview), 10 μm (zoom). scp - superior cerebellar peduncle, PBNel – lateral external parabrachial nucleus.

Figure 2. IL-6-immunoreactivity and GLP-1R-fluorescence and mRNA partially overlap in PBNel

Figure 2 shows overlap between cells with GLP-1R-RFP-immunoreactivity (green) and cells with IL-6-immunoreactivity (red). Cell nuclei (blue) are stained by DAPI. Shown are an overview of PBN (A) and a magnification of the indicated part of PBNel (B). Yellow arrowheads show examples of co-localization, whereas red arrowheads show examples of cells with only IL-6 immunoreactivity (B). Cell counting showed that 80% of GLP-1R containing cells also contained IL-6, whereas 44% of IL-6-immunoreactive cells also contained GLP-1R (C-D). The RNA scope technique showed a partial overlap between GLP-1R (red) and IL-6

(green) probes (E-F) in the external lateral part of the PBN, PBNel. Magnifications show examples of cells expressing both GLP-1R and IL-6, as well as examples of cells expressing only IL-6 (F I-III).
Confocal micrographs were obtained and cell counting was performed as described in Materials and Methods. Scale bars 80 μm (overview), 10 μm (zoom). scp - superior cerebellar peduncle, PBNel – lateral external parabrachial nucleus.

Figure 3. Intraperitoneal injection of Ex-4 increases the proportion of -IL-6-containing cells in PBNel of the RedIL6 reporter mouse

Figure 3 shows cells containing IL-6 in the PBNel as indicated by the mKATE2-IL-6 (RedIL6) reporter mouse (red) after intraperitoneal injection of Ex4 (A-B) or vehicle (C-D). Shown are overviews of PBN (A, C) and magnifications of the indicated parts of PBNel (B, D). Red arrowheads indicate examples of IL-6 containing cells (B, D). Cell counting shows that there is a marked increase in IL-6 containing cells in PBNel, as indicated by the mKATE2-IL-6 reporter mouse, after Ex4 injection (44%) as compared with vehicle (13%). In contrast, there is no difference in IL-6 containing cells in the lateral PBN excluding the PBNel (E).
Confocal micrographs were obtained and cell counting was performed as described in Materials and Methods. Scale bars 80 μm (overview), 10 μm (zoom). scp - superior cerebellar peduncle, PBNel – lateral external parabrachial nucleus.

Figure 4. Intraperitoneal injection of Ex-4 moderately increases CGRP-immunoreactivity in PBNel

Figure 4 shows and CGRP-immunoreactivity (green) after intraperitoneal injection of Ex4 (A-B) or vehicle (C-D). Shown are overviews of PBN (A, C) and magnifications of the indicated parts of PBNel (B, D). Green arrowheads indicate examples of CGRP-immunoreactive cells (B, D).
Cell counting shows a moderate increase in CGRP-immunoreactive PBNel-cells after Ex4 injection (31%) as compared with vehicle (24%). In contrast, there is no difference in CGRP containing cells in the lateral PBN excluding the PBNel (E).
Confocal micrographs were obtained and cell counting was performed as described in Materials and Methods. Scale bars 80 μm (overview), 10 μm (zoom). scp - superior cerebellar peduncle, PBNel – lateral external parabrachial nucleus, lPBN – lateral parabrachial nucleus.

Figure 5. Intraperitoneal injection of GDF15 does not increase the proportion of cells with IL-6 in PBNel as indicated with the RedIL6 reporter mouse

Figure 5 shows mKATE2-IL-6 (RedIL6) construct as an indicator of IL-6 content (red) after intraperitoneal injection of GDF15 (A-B) or vehicle (C-D). Shown are overviews of PBN (A, C) and magnifications of the indicated parts of PBNel (B, D). Red arrowheads indicate examples of IL-6 containing cells (B, D).
Cell counting shows that there is no difference in the proportion of IL-6 containing PBNel-cells between GDF15 (18%) and vehicle (17%) treated mice. Similarly, there is no difference in the lateral PBN excluding the PBNel (E). Confocal micrographs were obtained and cell counting was performed as described in Materials and Methods. Scale bars 80 μm (overview), 10 μm (zoom). scp - superior cerebellar peduncle, PBNel – lateral external parabrachial nucleus, lPBN – lateral parabrachial nucleus.

Figure 6. Intraperitoneal injection of GDF15 increases CGRP-immunoreactivity in PBNel

Figure 6 shows CGRP-immunoreactivity (green) after intraperitoneal injection of GDF15 (A-B) or vehicle (C-D). Shown are overviews of PBN (A, C) and magnifications of the indicated parts of PBNel (B, D). Green arrowheads indicate examples of CGRP-immunoreactive cells (B, D).
Cell counting shows an increase in CGRP-immunoreactive PBNel-cells after GDF15 injection (56%) as compared with vehicle (27%). In contrast, there is no difference in CGRP containing cells in the lateral PBN excluding the PBNel (E). Confocal micrographs were obtained and cell counting was performed as described in Materials and Methods. Scale bars 80 μm (overview), 10 μm (zoom). scp - superior cerebellar peduncle, PBNel – lateral external parabrachial nucleus, lPBN – lateral parabrachial nucleus.

Figure 7. Schematic representation of key findings of this study.

GDF15 produced outside CNS activates its newly discovered receptor, GFRAL in area postrema and NTS. Via a so far unknown mediator X, GDF15 then stimulates CGRP production in cells of the PBNel. GLP-1, produced in the NTS, increases IL-6 content in partly separate, non CGRP, cells of the PBNel. GLP-1 can also stimulate CGRP production slightly. GDF15 - Growth and differentiation factor 15, GFRAL - GDNF family receptor alpha like, CGRP - Calcitonin gene related peptide, PBNel - external lateral parabrachial nucleus, GLP-1 - glucagon-like peptide 1, IL-6 - interleukin-6.

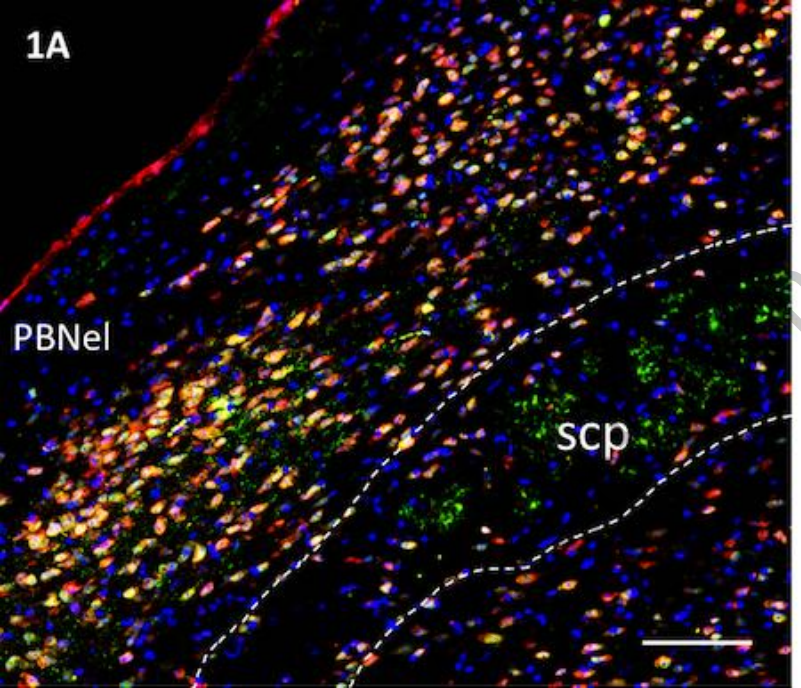

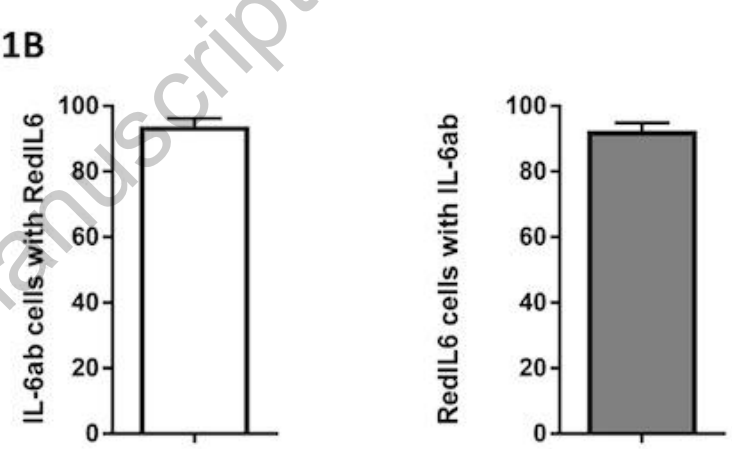

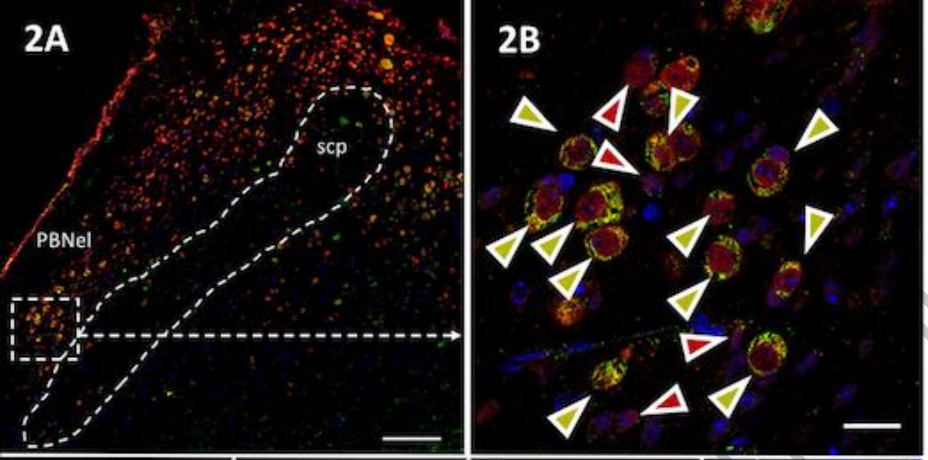

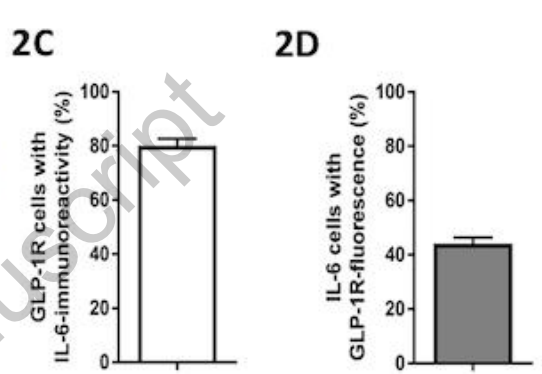

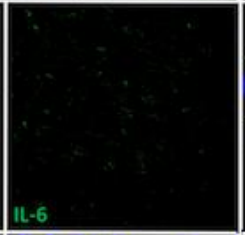

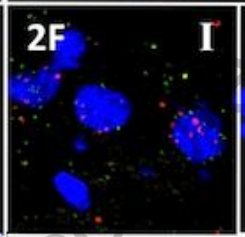

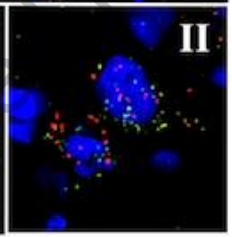

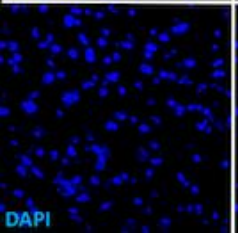

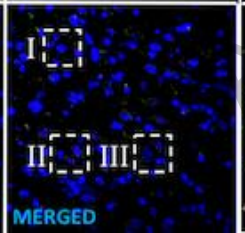

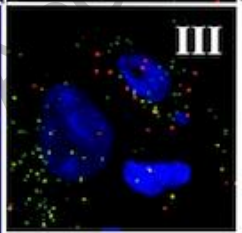

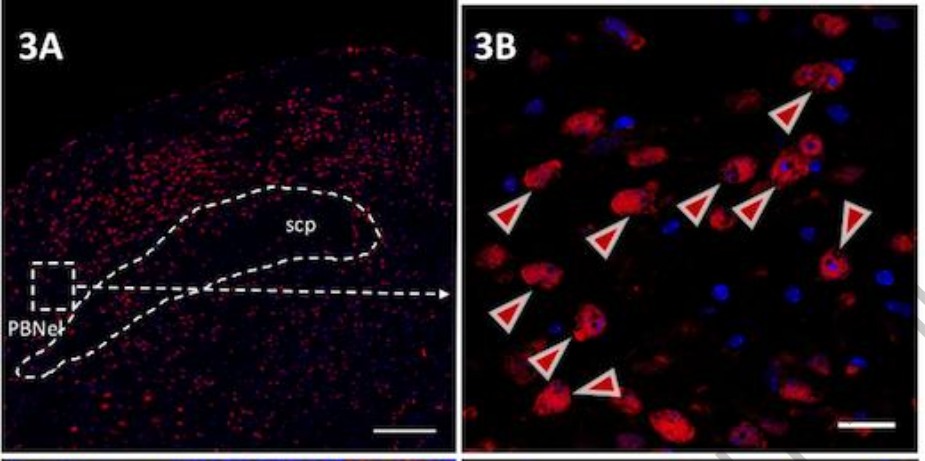

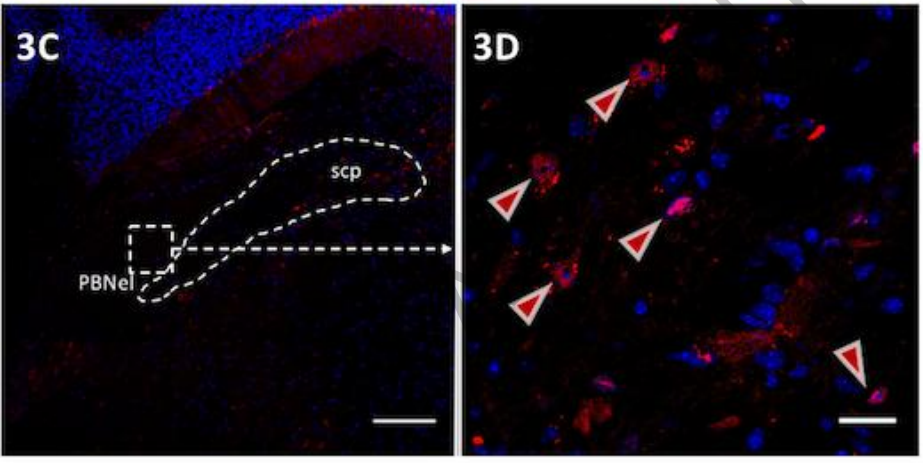

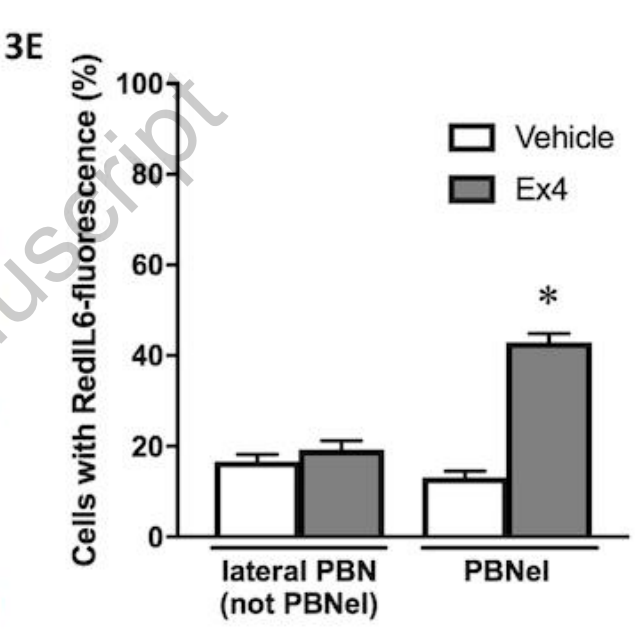

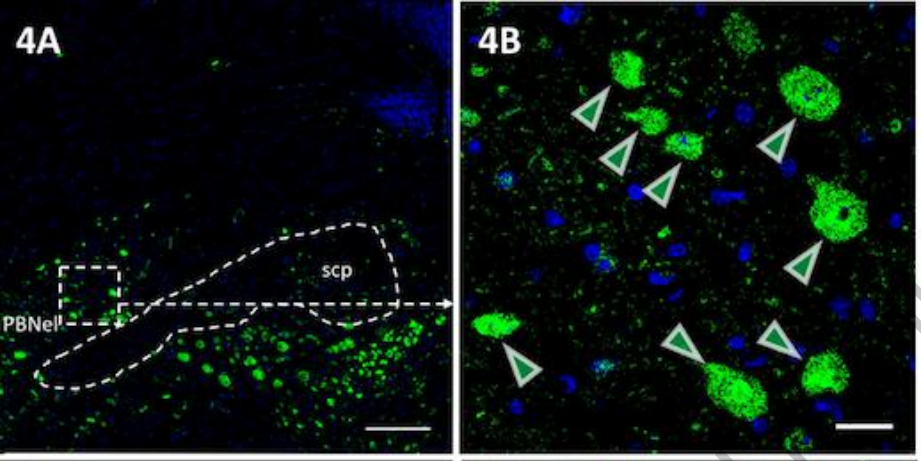

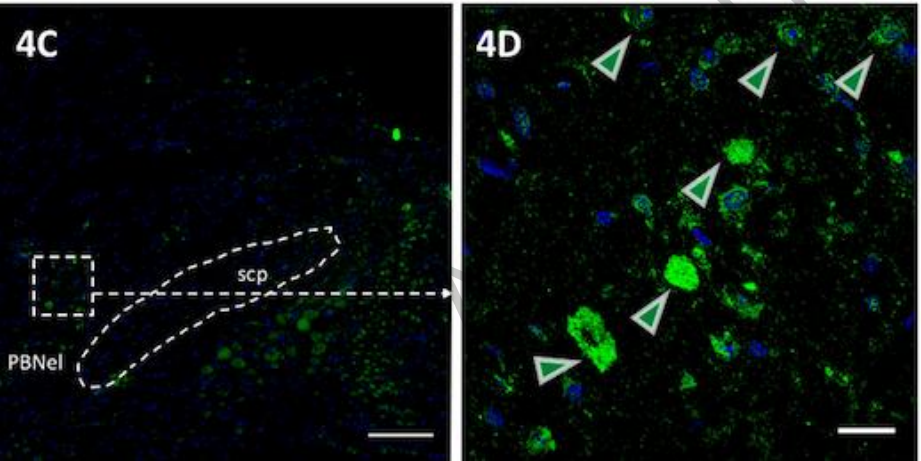

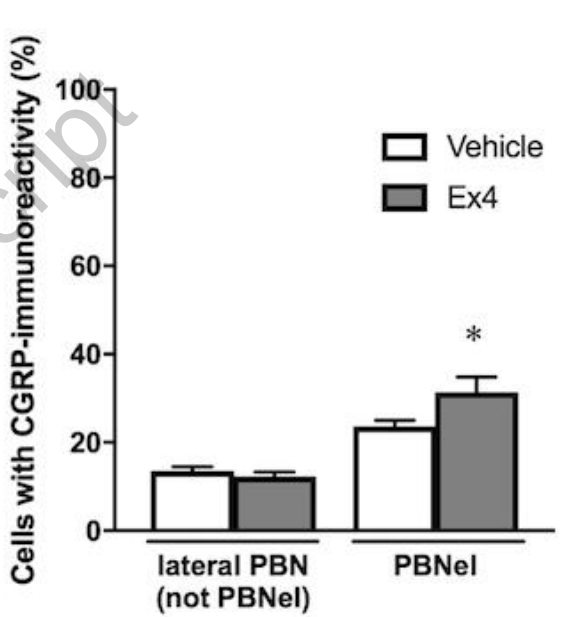

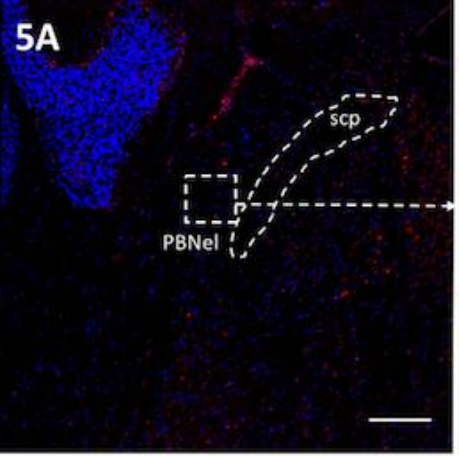

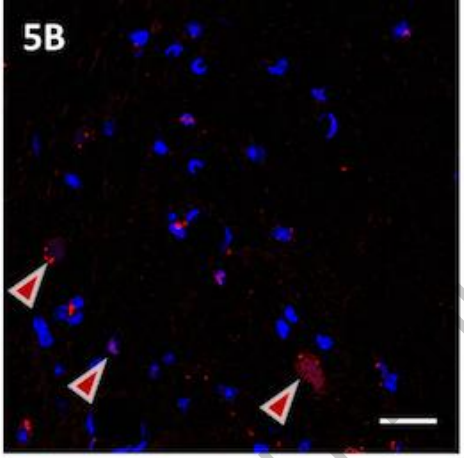

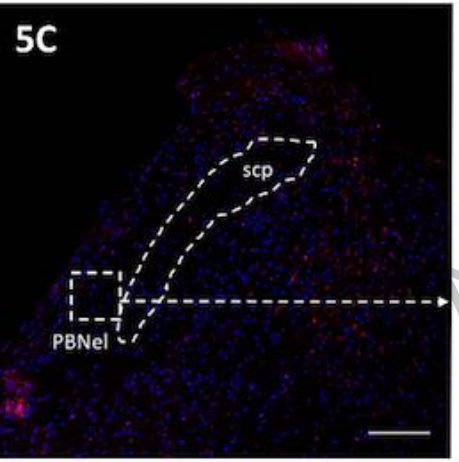

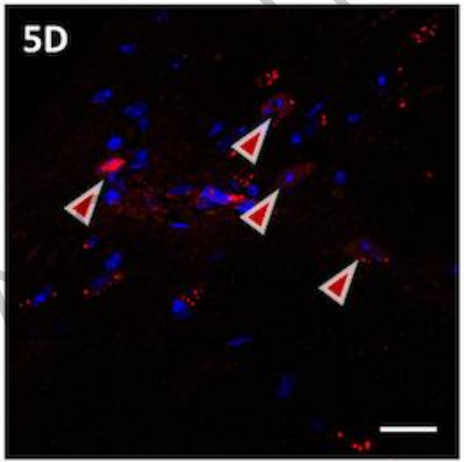

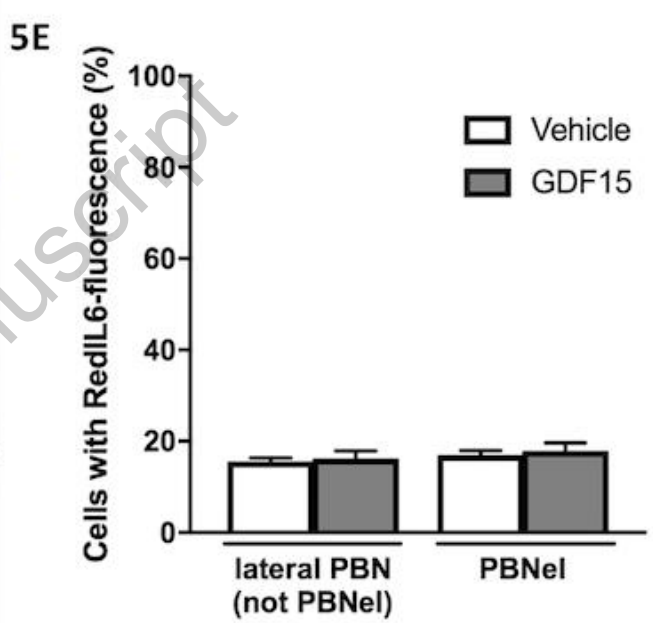

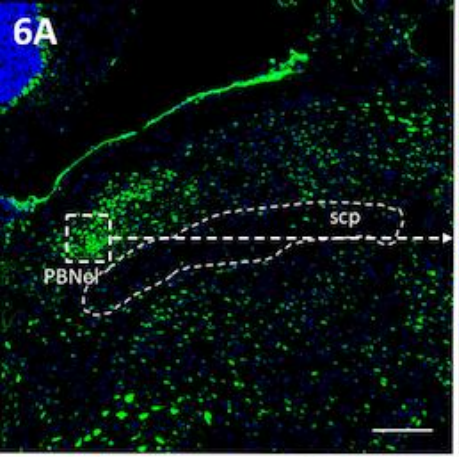

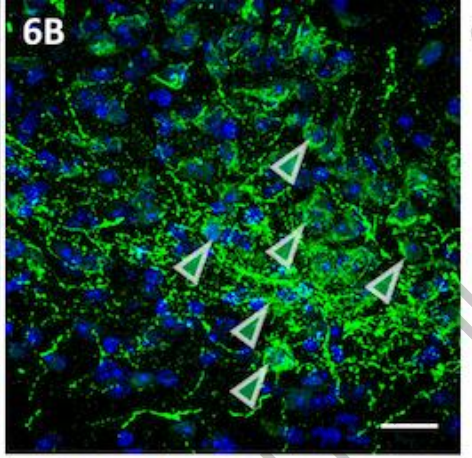

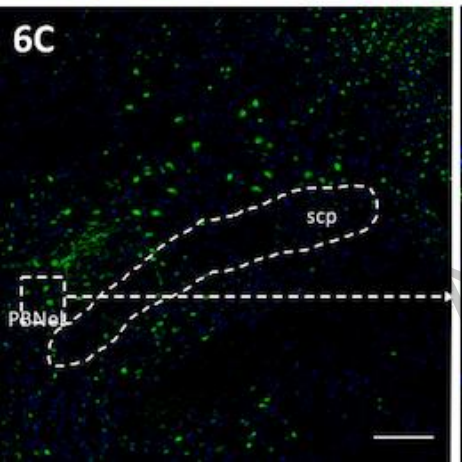

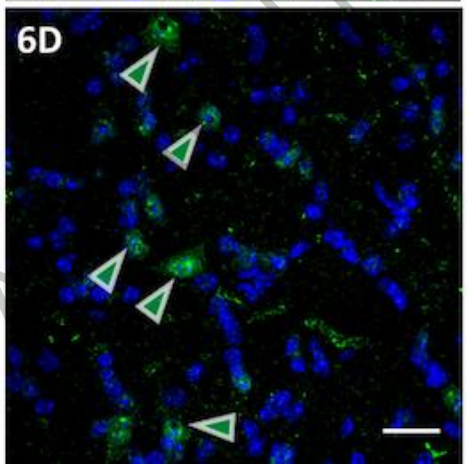

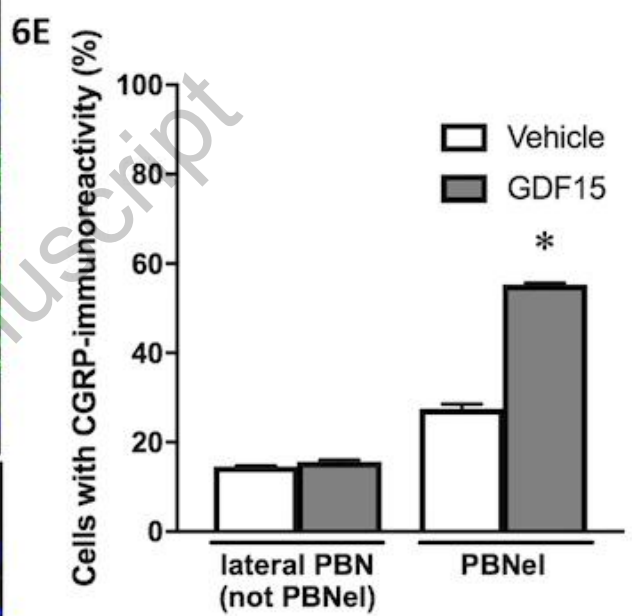

7

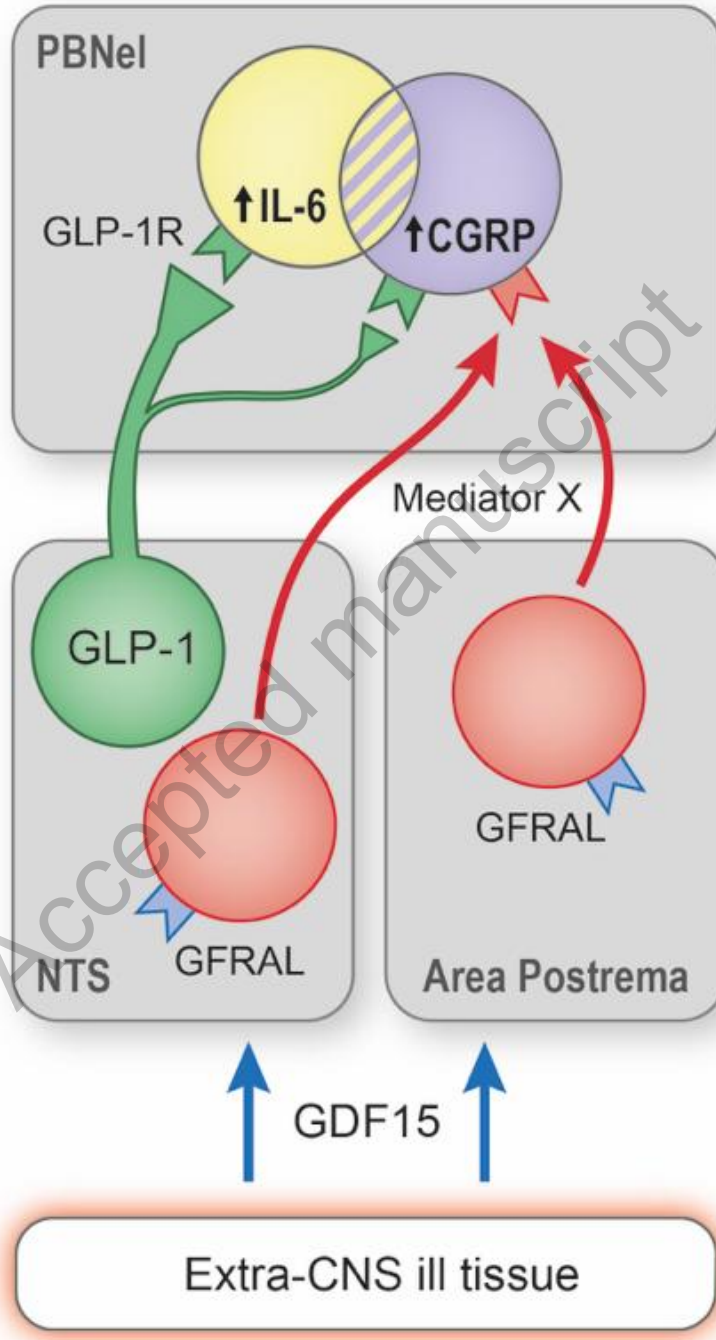

Antiserum	Dilution	Cat. No	Manufacturer	RRID
Rabbit anti-IL-6	1:200	SC-1265-R	Santa Cruz Biotechnology, Santa Cruz, CA, USA	AB_2011748
Mouse anti-RFP Tag	1:200	MA5-15257	ThermoFisher, Waltham, MA, USA	AB_10999796
Rabbit anti-RFP	1:200	R10367	ThermoFisher, Waltham, MA, USA	AB_2315269
Goat anti-CGRP	1:200	Ab36001	Abcam, Cambridge, UK	AB_725807
Goat anti-mouse Alexa fluor 488	1:250	A-11001	ThermoFisher, Waltham, MA, USA	AB_2534069
Goat anti-mouse Alexa fluor 568	1:250	A-11031	ThermoFisher, Waltham, MA, USA	AB_144696
Donkey anti-goat Alexa fluor 488	1:250	A-11055	ThermoFisher, Waltham, MA, USA	AB_2534102
Goat anti-rabbit Alexa fluor 568	1:250	A-11036	ThermoFisher, Waltham, MA, USA	AB_143011

Table 1. List of antibodies used in this paper.

Generation of IL-6 reporter mKATE2 mice

Targeting plan

A red fluorescent protein mKate2 was inserted into Il6 locus (Fig. S1), exactly located after translation start site, ATG.

Fig. S1. Il6 mKate2 report mice targeting strategy: A red fluorescent protein mKate2 was inserted into Il6 locus, and it is directly after translation start site, ATG.

Targeting construct

BAC clones (RP23-121M2 and RP24-172N24) containing mouse Il6 gene were obtained from BACPAC Resources Center (Children's Hospital Oakland Research Institute, Oakland (CHORI), California, USA). A 7550 bp fragment of Il6 gene containing exons 1, 2 and 3 was subcloned into the minimal vector, pACYC177 (New England Biolabs, MA, USA) by Red/ET recombination method according to the manufacturer's instructions (Gene Bridges GmbH, Germany). PCR product used in subcloning was amplified from pACYC177 plasmid using the primers
(A) 5'-CTCAGTTGGCACTGAATATACAGAATGACACTGCACCTTCACACGTGCAG GCAGACCTCAGCGCTAG -3'and (B) 5'- GTACATGAAGAACAACTTAAAAGATA ACAAGAAAGACAAAGCCAGAGTCTGAAGACGAAAGGGCCTC -3' where homology arms to 5' flanking region of exon 1 (primer A) and 3' untranslated region (primer B) of the Il6 gene are indicated in bold, and PCR primers for an ampicillin resistance (amp) gene and ori in pACYC177-plasmid are in italics. A mammalian expression vector encoding for red fluorescent protein mKate2, pmKate2-N vector was purchased from Evrogen (Evrogen JSC, Moscow, Russia). Neo resistant gene flanked with two loxP sites (loxP-PGK-Neo-loxP cassette, Gene Bridges) was introduced into pmKate2-N vector with In-Fusion® HD cloning kit (Clontech, CA, USA) according to the manufacturer's instructions. Finally, the replacement of partial exon 1, exons 2 and 3 and intron 1 and 2 of Il6 gene with mKate2 and Neo cassette containing 50 bp Il6 homology arms amplified by PCR was carried out by Red/ET recombination method. Primers were (C)
5'- GTAGCTCATTCTGCTCTGGAGCCCACCAAGAACGATAG TCAATTCCAGAAACCGCTATGGTGAGCGAGCTGATTAAGG and (D) 5'- ATAGCACTGGTTGGTAAACTTTCCCTCACCCTAGCAGCTGCTGAGGTACC GCGGATTTGTCCTACTCAGG -3' where homology arms to the Il6 gene are indicated in bold and PCR primers for mKate2 and Neo cassette are shown in italics. Validity of final targeting construct was confirmed by restriction enzyme digestion and sequencing.

Gene targeting in ES cells

G4 embryonic stem cells (derived from mouse 129S6/C57BL/6Ncr) were cultured on neomycin-resistant primary embryonic fibroblast feeder layers, and 10^6 cells were electroporated with 30 ug of linearized targeting construct. After electroporation, the cells were plated on 100-mm culture dishes and exposed to G418 (300 ug/ml; Sigma). Colonies (192) were picked up after 7-9 days selection and grown on 96-well plate. In order to delete Neo cassette in the targeted ES cells, and targeted ES cells were re-electroporated

with plasmid, pCAGGS-Cre. After electroporation, the cells were plated on 100-mm culture dishes and colonies were picked up after 3-5 days growth, and grown on 96-well plate.

Screening of targeted ES clones

DNA isolated from ES cell clones was screened by long-range (LR) - PCR for both 5' and 3' homologous arms. PCR products with 5' homologous arm, 3054 bp fragment was generated with a primer pair corresponding to 5' flanking region of 5' homologous arm (IL65HaUF1: TAGTAGAAGCTCAAGCTCTGGG) and to mKate2 gene (mKate2AntiSense2: GGTGTGGTTGATGAAGGTTT), and PCR product with 3 homologous arm, 3731 bp fragment was generated with primer pair corresponding to Neo gene (Neogenese1: CCTCGTGCTTTACGGTATCG), and 3' flanking region of 3' homologous arm (IL63HaDR2: GCTCTCATAATGGGTGACTATG).

Total 192 clones were picked up and screened by LR-PCR. Two clones contained both 5' and 3' homologous arm, 3054, and 3731 bp fragments in PCR analysis (Fig. S2). Correct PCR products were verified by sequencing.

Fig. S2. Representative positive ES clone was found to contain homologous recombination of Il6 by LR-PCR screening using the primer pairs, Il6Arm5UF1 and mKate2Antisense2, Neogenese1 and Il6Arm3DR2.

In order to detect targeted ES clones with Neo deletion after Cre recombination, DNA isolated from ES cells re-electroporated with plasmid, pCAGGS-Cre were screened by PCR with several different primer pairs. Several correct clones were found from 48 clones. The right clones were further confirmed by sequencing.

Blastocyst injection

The targeted ES cells with Neo deletion were injected into C57BL/N6 mouse blastocysts to generate chimeric mice. Germline transmission was achieved by cross-breeding male chimeras with C57BL/N6 females. C57BL/6N mice used as blastocyst donors were obtained from Charles River Laboratories (Willmington, MA). The mice were maintained in a specific pathogen free stage at Central Animal Laboratory at the University of Turku. All studies carried out with the mice were approved by The Finnish ethical committee for experimental animals, complying with international guidelines on the care and use of laboratory animals.

DNA extraction and genotyping

Genotyping of the mice was carried out with DNA extracted from the ear marks of 2-week-old mice. Genotyping was performed as follows:

Table S1. Genotype Protocol of Il6-mKate KI Mice (TUKO62) (TCDM, ZHANG FP)

Combined RNA Scope and immunohistochemistry

In-situ hybridization (RNA Scope) was performed as described in Materials and Methods with the following changes: The mouse IL-6 mRNA probe (Mm-Il6 315891), positive- (Mm-Ppib 213911) and negative controls (DapB 310043) were stained with cy3. Brain slices from four heterozygous RedIL6 mice were used. Following the last step in this protocol, slides were incubated overnight with anti-RFPtag (Table 1) in normal goat serum. The following day slides were washed 3x5 min in TNT buffer, followed by 1h incubation with Alexa488 anti-mouse (Table 1). Slides were washed 3x5 min in TNT buffer and cell nuclei were stained with DAPI followed by another 3x5 min wash. Slides were then mounted with ProLong Diamond Antifade and coverslipped. Micrographs were developed using the lsm700 system.

Figure S3. Representative confocal micrograph of combined RNAscope and immunohistochemistry showing high co-localization between IL-6 mRNA (cy3, red) and RedIL6 (Alexa 488, green) fluorescence in PBNel (B). Cell nuclei stained by DAPI (blue). Examples of individual cells where IL-6 mRNA and RedIL6 is co-localized shown in (C).

Figure S4. IL-6 ab immunohistochemistry (green) in wt (A) and homozygous RedIL6 mice (B). Cell nuclei stained by DAPI (blue). The IL-6 ab used in this paper shows markedly less staining in homozygous RedIL6 "IL-6 $^{-/-}$" mice. Scale bars – 100 μm. scp – superior cerebellar peduncle.

RedIL6 and CGRP immunohistochemistry

Figure S5A. RedIL6 (red) and CGRP (green) immunoreactivity partially overlaps in the PBNel. Cell nuclei stained by DAPI (blue). Examples of RedIL6 (red arrowheads), CGRP-immunoreactive cells (green arrowheads) and co-localization (yellow arrowheads). Scale bar – 10 μm.

Figure S5B. About 40% of all CGRP-immunoreactive cells also show RedIL6-fluorescence and vice versa.

Figure S6. Representative confocal micrographs of cells containing IL-6 in the PBNel as indicated by the mKATE2-IL-6 (RedIL6) reporter mouse (red) 60 min after intraperitoneal injection of Ex4 (A-B) or vehicle (C-D). Shown are overviews of PBN (A, C) and magnifications of the indicated parts of PBNel (B, D). Red arrowheads indicate examples of IL-6 containing cells (B, D). Cell counting shows that there is a marked increase in IL-6 containing cells in PBNel, as indicated by the mKATE2-IL-6 reporter mouse, after Ex4 injection as compared with vehicle (E). In contrast, there is no difference in IL-6 containing cells in the lateral PBN excluding the PBNel (E).

Confocal micrographs were obtained and cell counting was performed as described in Materials and Methods. Scale bars 80 μm (overview), 10 μm (zoom). scp - superior cerebellar peduncle

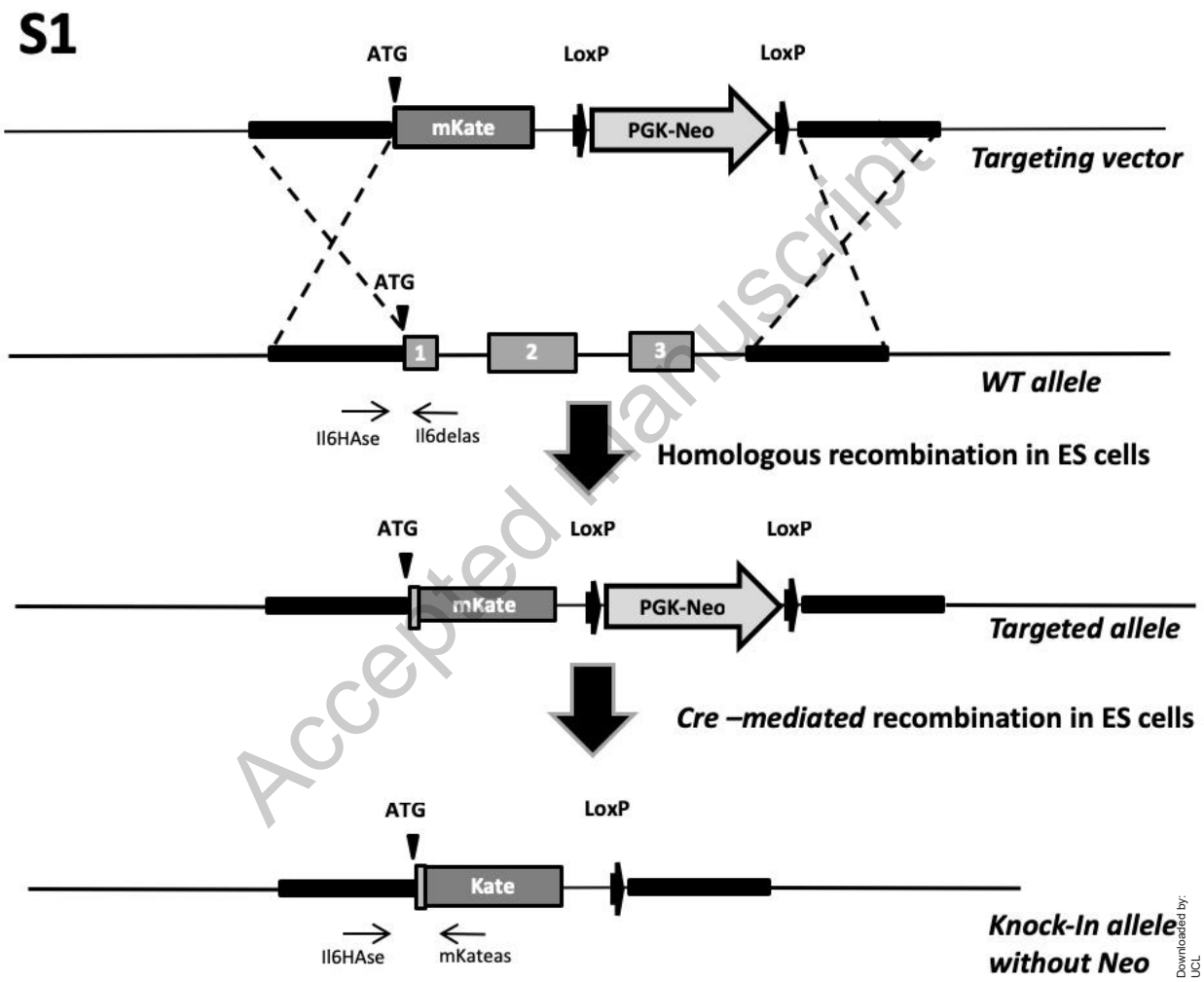

S2

S3A

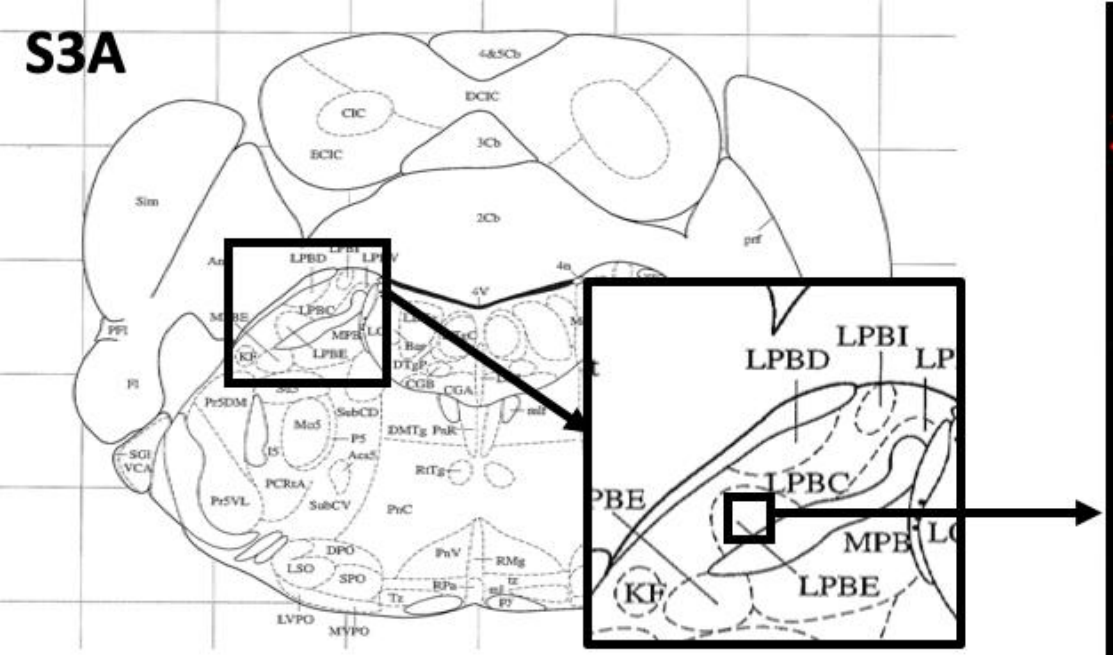
4&5Cb
DCIC
CIC
ECIC
3Cb
Sim
2Cb
prf
LPBD
LPBI
LPBC
MPB
LPBE
KF
4V
PPT
Fl
Bar
DTgP
CGB
CGA
Pr5DM
SubCD
Mo5
P5
DMTg
PnR
SGl
VCA
I5
Acs5
RtTg
PCRtA
Pr5VL
SubCV
PnC
DPO
PnV
RMg
LSO
SPO
RPa
Tz
P7
LVPO
MVPO
LPBD
LPBI
LP
LPBC
PBE
MPB
LPBE
KF

S3B

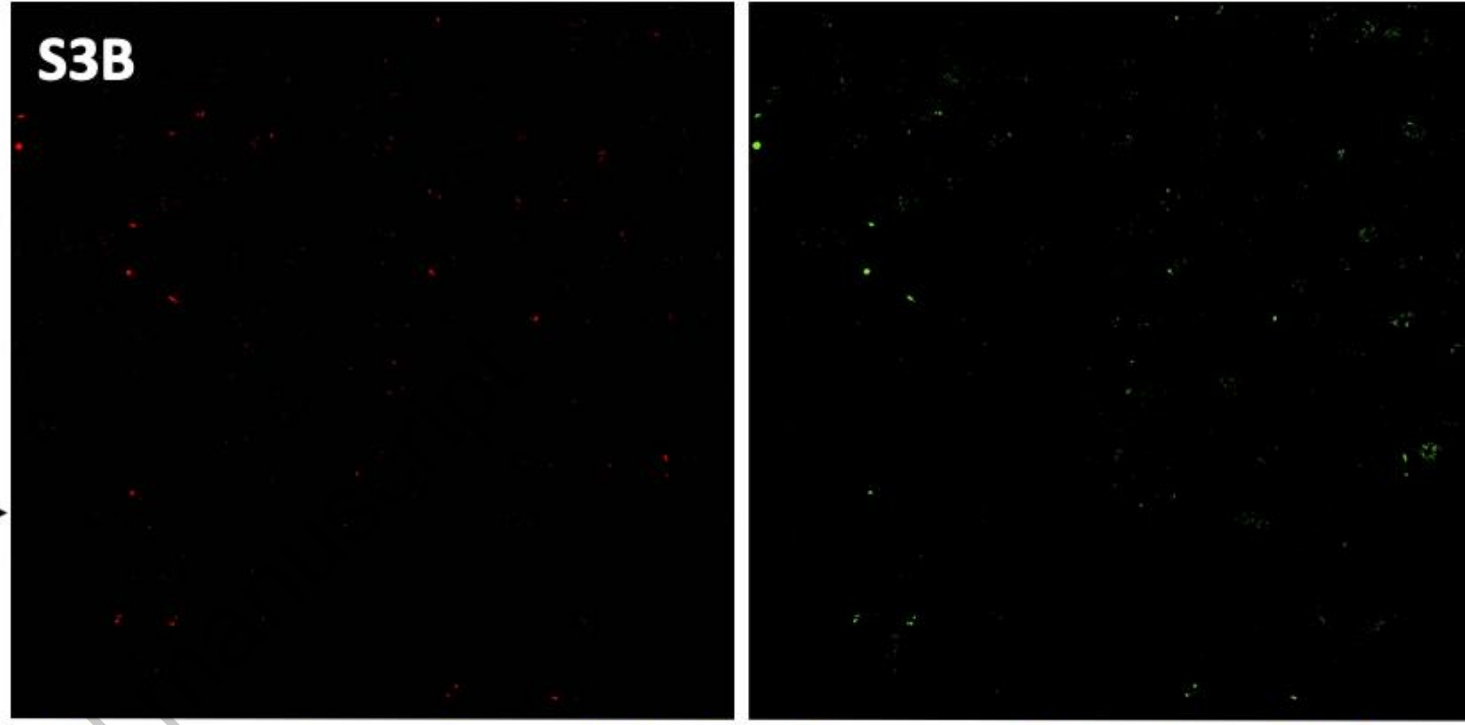

S3C

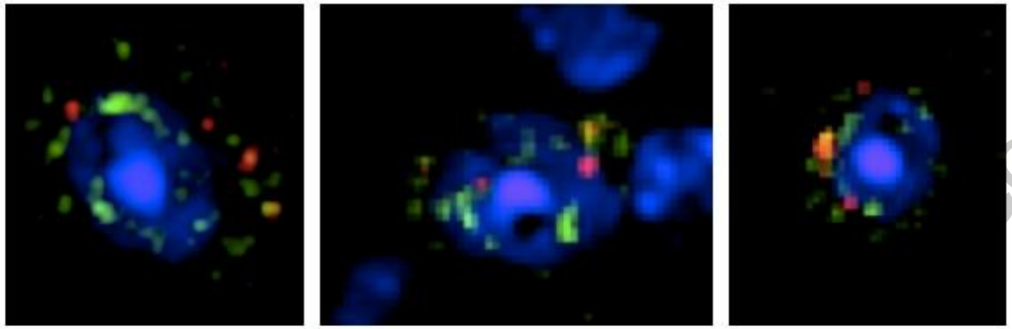

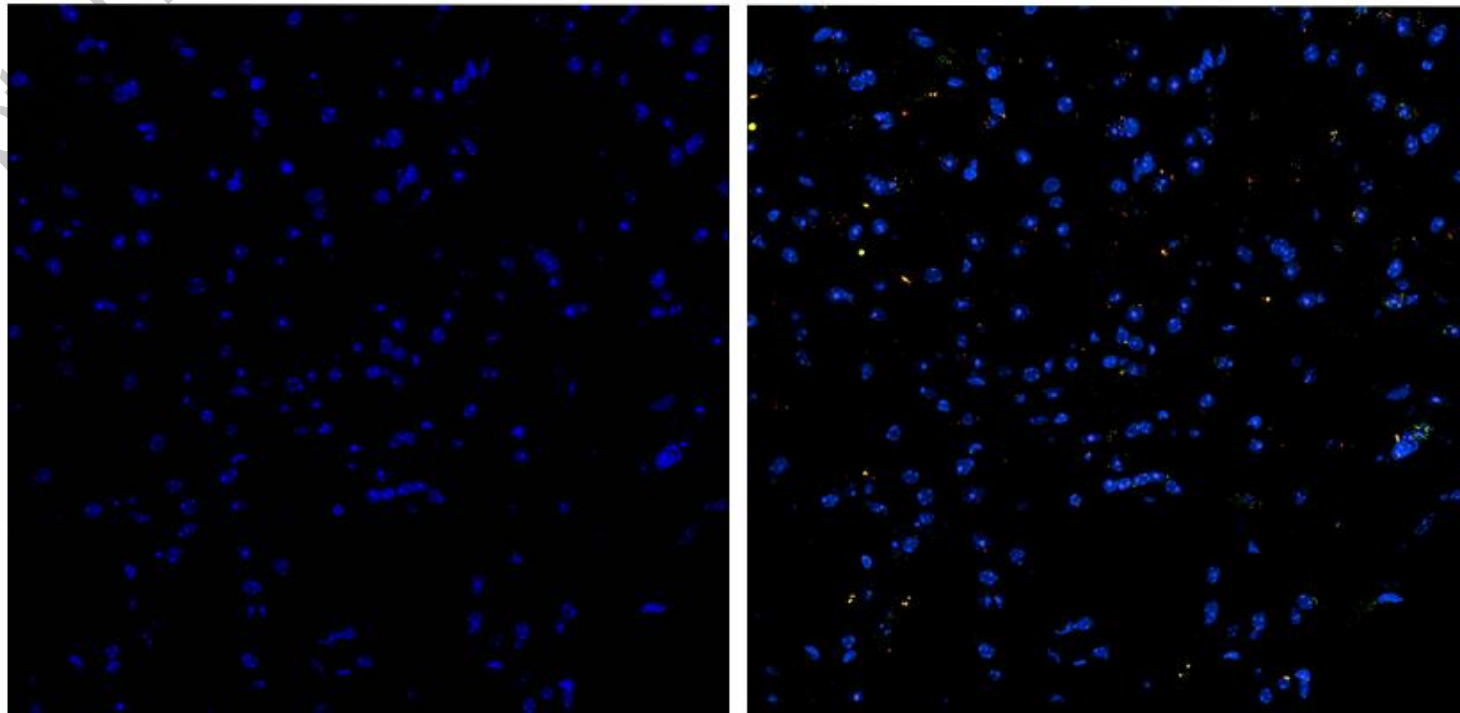

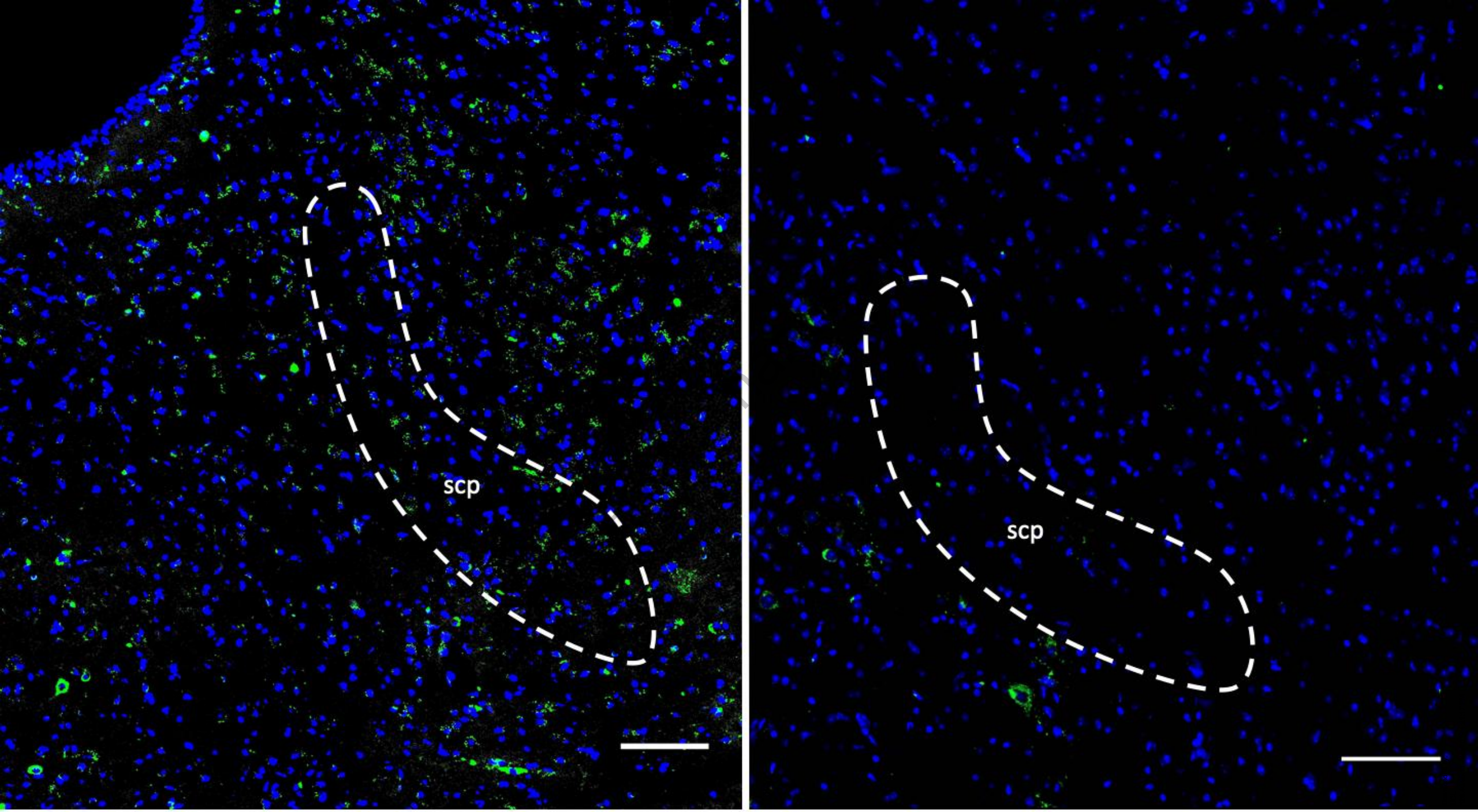
scp
scp

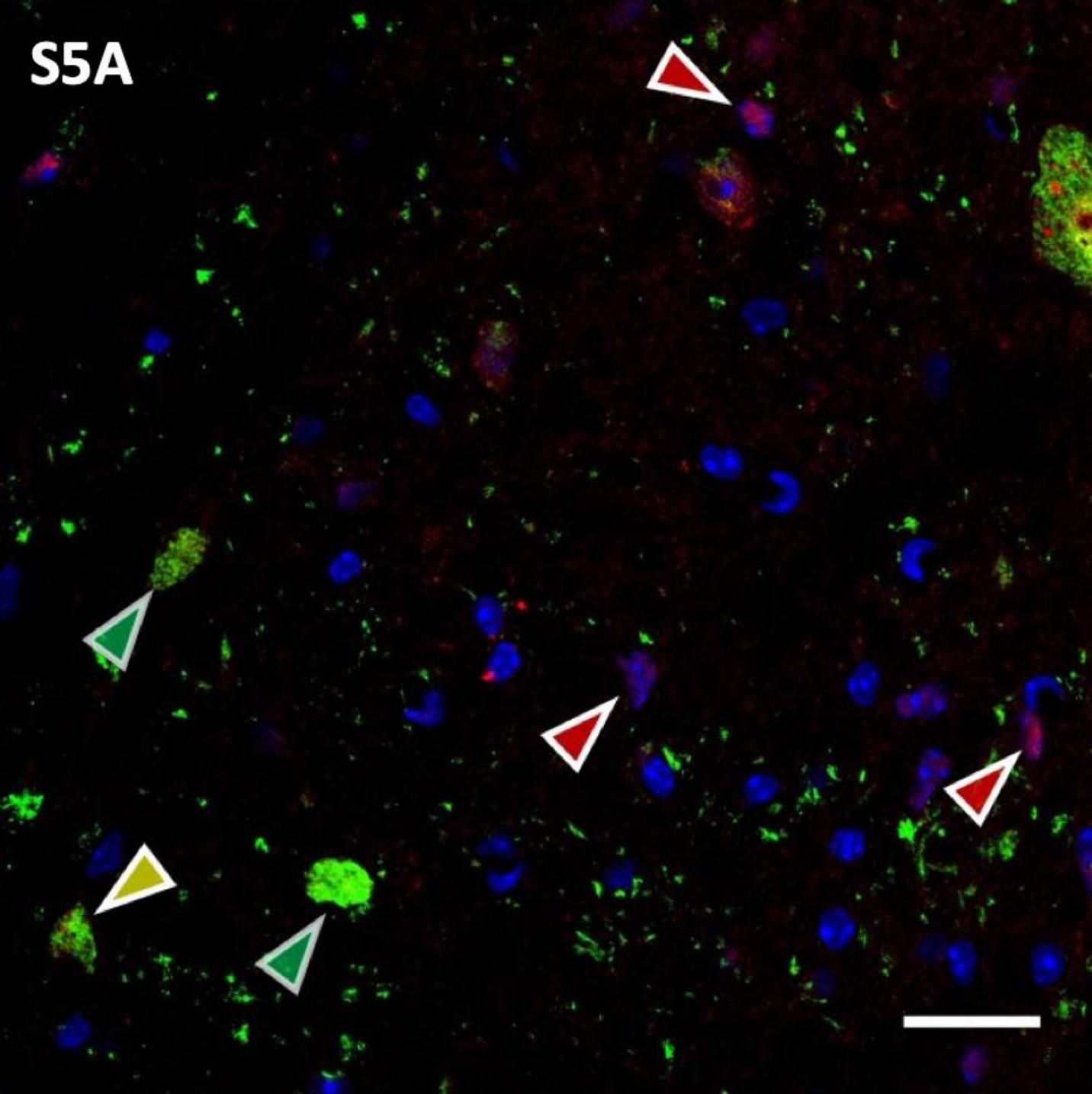
S5A

S5B

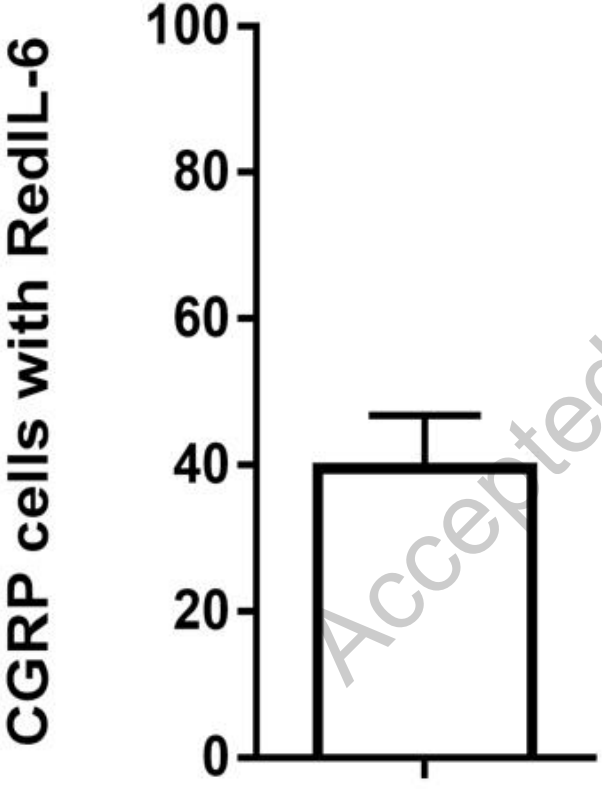

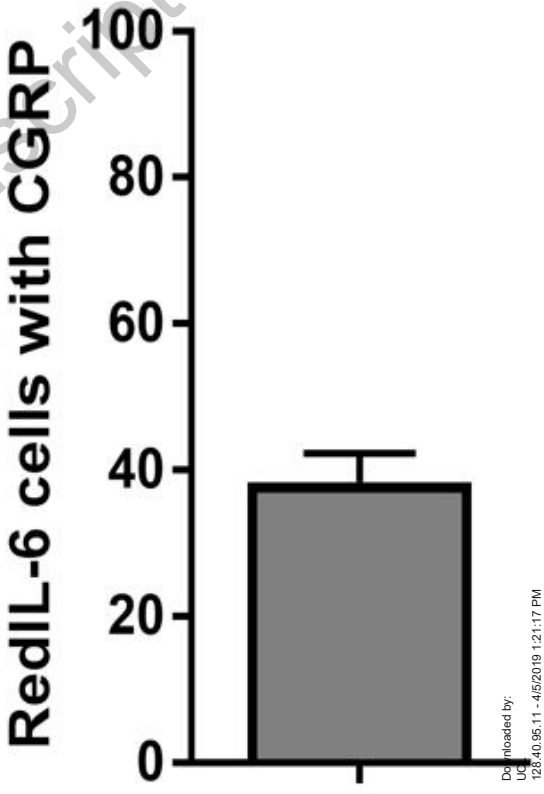

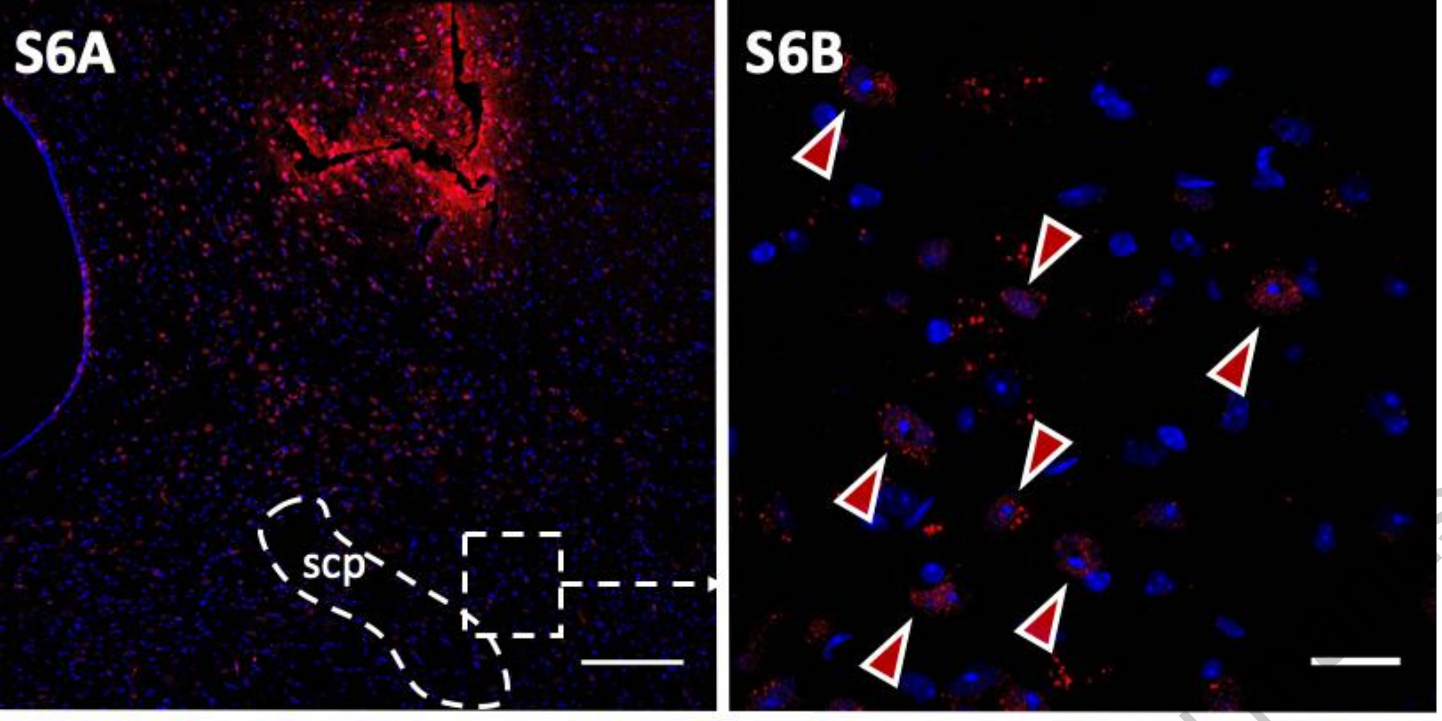

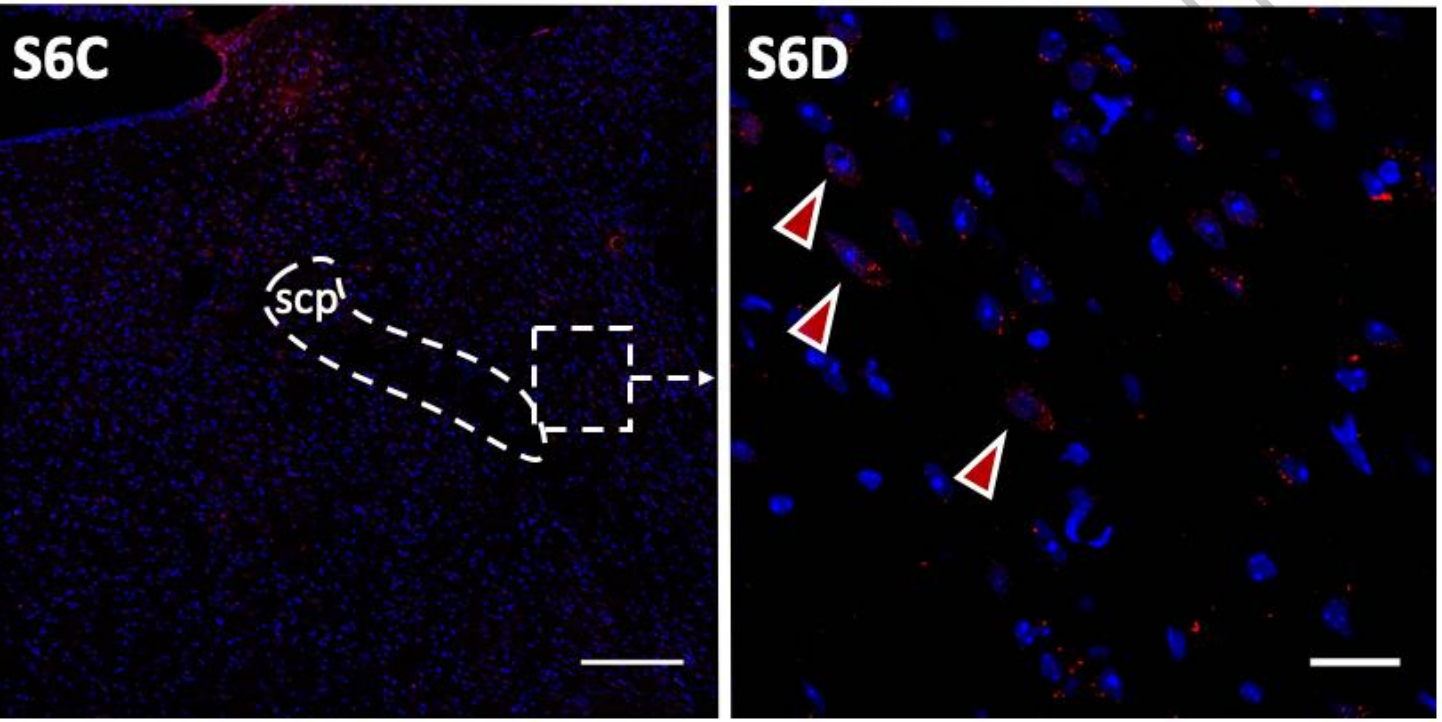

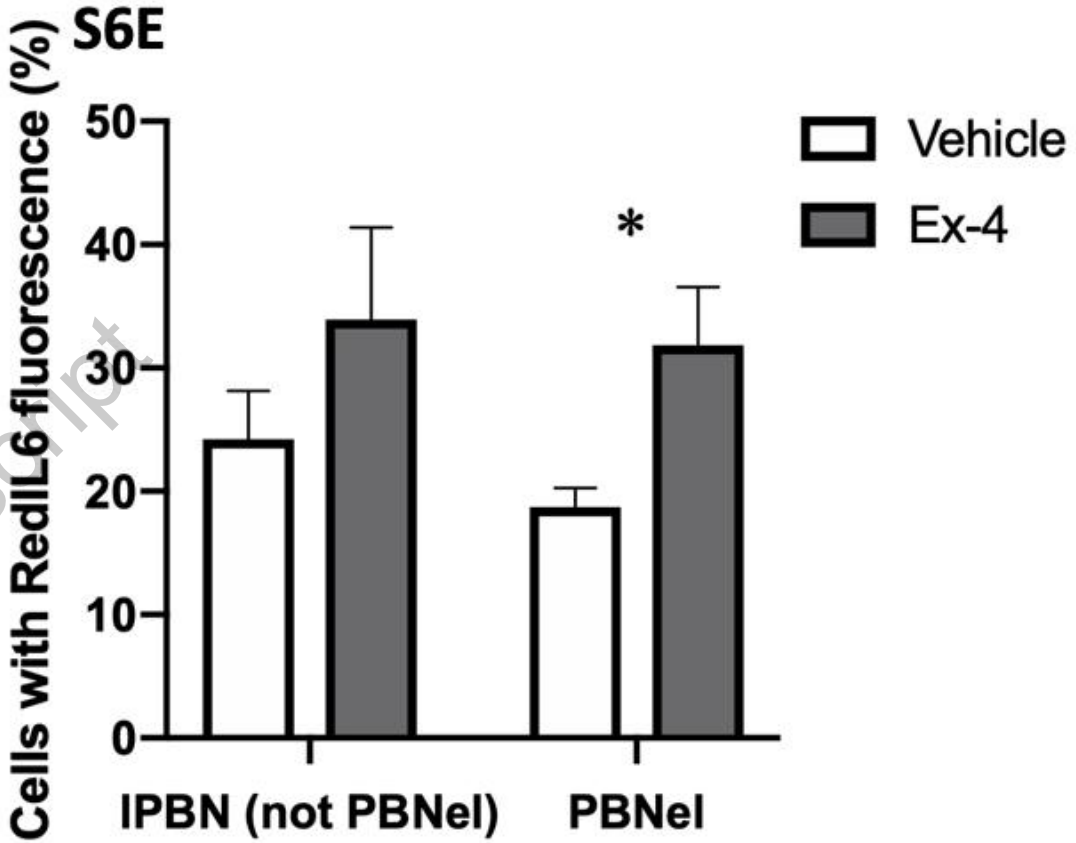

Primer pairs:	WT (bp)	HEZ(+/KI) (bp)	HOZ(KI/KI)(bp)
1. Il6HA5se1 +Il65HADR1	435	435	
2. Il63HAUF2 + Il6HA3As1	308	308	
3. mKate2sense2 + Il6HA3As1		448	448
4. Il6HA5se1 +mKate2As2		456	456

PCR reaction components:

Final concentration
Genomic DNA x ug
10x polymerase buffer 5 ul
5 mM dNTP mix 2 ul
Forward primer (10 pmol/l) 2 ul
Reverse primer (10 pmol/l) 2 ul
DNA polymerase 1 ul
H_2O x ul
Total volume 50 ul

PCR reaction condition

1. Initial denaturation 96°C 3 min
2. Denaturation 96°C 30 sec
3. Annealing 56°C 30 sec
4. Extension 72°C 1 min
5. Back to step 2 for 35 cycles
6. Final extension 72 C 10 min
7. Hold 4°C

Primer sequences:

1. Il6HA5se1: GATTCTTTCGATGCTAAACG
2. Il6HA3As1: TCTAACACCTCAAAGCCAAG
3. Il65HADR1: CAACTGGATGGAAGTCTCCTGC
4. Il63HAUF2: ACTGGATATAATCAGGTAGAAACTTGTC